Neuroanatomy of the killer whale (Orcinus orca): a magnetic resonance imaging investigation of structure with insights on…

6 authors, including:

CrossMark

ORIGINAL ARTICLE

Neuroanatomy of the killer whale (*Orcinus orca*): a magnetic resonance imaging investigation of structure with insights on function and evolution

Alexandra Wright[1] · Miriam Scadeng[2] · Dominik Stec[2] · Rebecca Dubowitz[2] · Sam Ridgway[3] · Judy St. Leger[4]

Abstract The evolutionary process of adaptation to an obligatory aquatic existence dramatically modified cetacean brain structure and function. The brain of the killer whale (*Orcinus orca*) may be the largest of all taxa supporting a panoply of cognitive, sensory, and sensorimotor abilities. Despite this, examination of the *O. orca* brain has been limited in scope resulting in significant deficits in knowledge concerning its structure and function. The present study aims to describe the neural organization and potential function of the *O. orca* brain while linking these traits to potential evolutionary drivers. Magnetic resonance imaging was used for volumetric analysis and three-dimensional reconstruction of an in situ postmortem *O. orca* brain. Measurements were determined for cortical gray and cerebral white matter, subcortical nuclei, cerebellar gray and white matter, corpus callosum, hippocampi, superior and inferior colliculi, and neuroendocrine structures. With cerebral volume comprising 81.51 % of the total brain volume, this *O. orca* brain is one of the most corticalized mammalian brains studied to date. *O. orca* and other delphinoid cetaceans exhibit isometric scaling of cerebral white matter with increasing brain size, a trait that violates an otherwise evolutionarily conserved cerebral scaling law. Using comparative neurobiology, it is argued that the divergent cerebral morphology of delphinoid cetaceans compared to other mammalian taxa may have evolved in response to the sensorimotor demands of the aquatic environment. Furthermore, selective pressures associated with the evolution of echolocation and unihemispheric sleep are implicated in substructure morphology and function. This neuroanatomical dataset, heretofore absent from the literature, provides important quantitative data to test hypotheses regarding brain structure, function, and evolution within Cetacea and across Mammalia.

✉ Alexandra Wright
awright@ucsd.edu; alexandrakwright@gmail.com

[1] Center for Marine Biotechnology and Biomedicine, Scripps Institution of Oceanography, University of California, San Diego, La Jolla, CA 92093, USA

[2] Center for Functional MRI, Department of Radiology, University of California, San Diego, La Jolla, CA 92093, USA

[3] National Marine Mammal Foundation, San Diego, CA 92106, USA

[4] SeaWorld San Diego, 500 SeaWorld Drive, San Diego, CA 92109, USA

Introduction

Many species of Cetacea (whales, dolphins, and porpoises) possess exceptionally large brains characterized by distinct structural and diverse neuronal morphology (Oelschläger and Oelschläger 2009; Butti et al. 2014a), unique cortical topography (Ladygina et al. 1978), and unparalleled gyrencephaly (Manger et al. 2012). Cetacean species of the superfamily Delphinoidea, a group comprising the Delphinidae and their relatives, attain some of the largest relative brain sizes among extant mammals, which are comparable to and in some cases surpass that of nonhuman anthropoid primates (Marino 1998; Marino et al. 2004a;

Ridgway and Brownson 1984). Delphinoid brain size evolution may be driven by developmental prolongation, increased information-processing demands imposed by complex social systems, or obligate existence within the marine environment. Global enlargement of the delphinoid brain may be associated with protracted pre- and postnatal development periods (Charvet and Finlay 2012; Whitehead and Mann 2000) characterized by prolonged maternal investment (i.e., gestation and lactation phases; Barton and Capellini 2011; Whitehead and Mann 2000) that serve to extend the duration of neuronal and glial cell production (Charvet et al. 2011). Selection for enhanced social cognition permitting behavioral flexibility to negotiate interactions with conspecifics may also be associated with delphinoid encephalization (Connor 2007; Dunbar 1998; Shultz and Dunbar 2006). Alternatively, or additionally, the large size of the delphinoid brain may be attributed to hypertrophy of neural structures that mediate acoustic processing of echolocation and communication signals and acousticomotor integration (Ridgway 1986, 1990, 2000; Oelschläger 2008; Hanson et al. 2013). The ability of delphinoid cetaceans to rapidly integrate and process auditory stimuli is critical for prey detection, predator avoidance, navigation, and communication with conspecifics in the marine environment, where sound transmission is considerably faster than in air and alternate reliable sensory input is limited (Oelschläger 2008; Au and Nachtigall 1997; Tyack 1999; Wartzok and Ketten 1999).

Quantitative examination of the hypertrophy, regression, or loss of neural structures using magnetic resonance imaging (MRI) may provide functional and evolutionary insights into delphinoid neuroanatomy. MRI has been used to examine the neuroanatomy of an assortment of delphinoids, including the Atlantic white-sided dolphin (*Lagenorhynchus acutus*; Montie et al. 2007, 2008), beluga whale (*Delphinapterus leucas*; Marino et al. 2001a; Ridgway et al. 2002), bottlenose dolphin (*Tursiops truncatus*; Hanson et al. 2013; Ridgway et al. 2006; Marino et al. 2001c, 2004d), common dolphin (*Delphinus delphis*; Alonso-Farré et al. 2014; Haddad et al. 2012; Marino et al. 2001b, 2002; Berns et al. 2015; Oelschläger et al. 2007), harbor porpoise (*Phocoena phocoena*; Marino et al. 2003), killer whale (*Orcinus orca*; Marino et al. 2004b), pantropical spotted dolphin (*Stenella attenuata*; Haddad et al. 2012; Berns et al. 2015), spinner dolphin (*Stenella longirostris orientalis*; Marino et al. 2004c), and striped dolphin (*Stenella coeruleoalba*; Alonso-Farré et al. 2014). Also, studies implementing MRI for quantitative analysis and three-dimensional (3D) reconstruction of neuroanatomical structures have been performed in a range of delphinoid species of varying ontogeny (Hanson et al. 2013; Montie et al. 2008; Marino et al. 2001b, c, 2002, 2004c, d). However, detailed morphometric analysis of the neuroanatomy of *O.*

orca, the largest delphinoid cetacean, with possibly the most voluminous brain of all mammals (Ridgway and Hanson 2014), has not been conducted. To date, neuroanatomical assessments of *O. orca* have been limited in scope, encompassing descriptive studies of gross morphology (Marino et al. 2004b) and brain stem anatomy (De Graaf 1967) in addition to measurements of mass relationships (Ridgway and Brownson 1984; Ridgway and Hanson 2014; Ridgway and Tarpley 1996; Pilleri and Gihr 1970), mid-sagittal area of the corpus callosum (Tarpley and Ridgway 1994; Keogh and Ridgway 2008), callosal fiber composition (Keogh and Ridgway 2008), neuron number per cortical unit (Poth et al. 2005), and von Economo neurons (Hof and Van Der Gucht 2007). Consequently, acquisition of MRI-derived neuroanatomical measurements and a global 3D atlas of *O. orca* neuromorphology are important for expanding knowledge of *O. orca* brain structure and potential function, making cross-species comparisons within the Cetacea, and examining mammalian brain evolution.

Therefore, in this study, MRI-based measurements and 3D reconstructions of an *O. orca* brain, acquired while intact within the neurocranium, are presented. MR images were manually segmented into regions of interest (ROIs) for quantitative analysis and 3D volume rendering. ROIs encompass: (1) cortical gray and cerebral white matter, (2) subcortical nuclei (i.e., caudate nuclei, putamina, globi pallidi, and thalamic nuclei), (3) cerebellar gray and white matter, (4) corpus callosum, (5) hippocampi, (6) superior and inferior colliculi, and (7) neuroendocrine structures (i.e., pineal and pituitary glands). *O. orca* neuroanatomy is discussed as it relates to the evolutionary adaptations of delphinoid cetaceans to the marine environment and mammalian brain evolution with comparisons across taxa.

Materials and methods

Specimen

The specimen examined in this study was the in situ postmortem brain of a male 544 cm, 2368 kg *O. orca* aged 12 years. This *O. orca* was not yet physically mature compared to conspecifics in this population. The cause of death was acute intestinal volvulus (Begeman et al. 2012) and non-neurological in nature. On necropsy examination, the head was separated from the body at the atlanto-occipital joint (Fig. 1). The specimen was prepared for insertion into the 3 Tesla MR scanner bore (diameter: 60 cm) by removing soft tissues (i.e., cranial blubber, acoustic fat, muscle, and connective tissue) and reducing cranial bone by repeated cuts (Fig. 1). MRI was performed within 30 h of death.
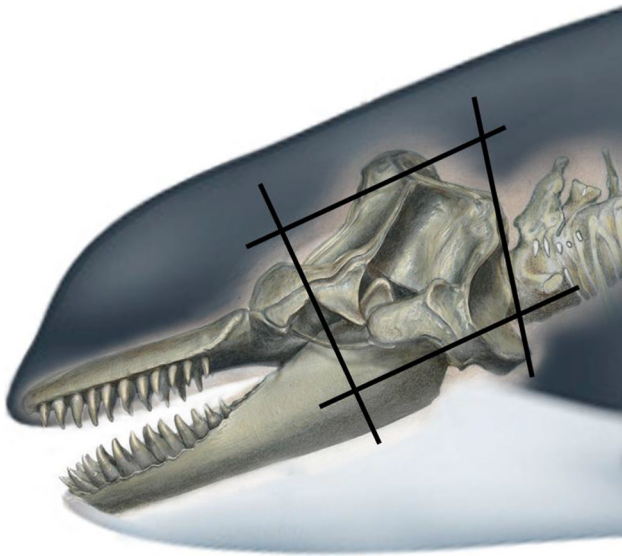
Fig. 1 *O. orca* head with superimposed cranium extending a few vertebrae beyond the atlanto-occipital joint. *Lines* indicate where cuts were made in preparing the specimen for MRI. Illustration by Sharon Birzer

Ethics statement

No live animals were used for this study. The *O. orca* specimen was examined opportunistically during postmortem investigation.

MRI protocol

The size of the specimen (width = 30.5 cm × height = 24.0 cm × anteroposterior length = 22.6 cm) was at the upper limits of the imaging capability of the body gradient coil of the MRI scanner, while allowing data collection as a single acquisition. MR images were acquired in the frontal plane with a 3 Tesla General Electric (GE) scanner (GE Medical Systems, Milwaukee, WI, USA) at the University of California, San Diego Center for Functional MRI. T2-weighted images were acquired using a 2D fast spin echo (FSE-XL) imaging sequence with the following protocol parameters: echo time (TE) = 48 ms; repetition time (TR) = 6000 ms; inversion time (TI) = 450 ms; 10 averages; field of view = 48 × 48 cm; in-plane matrix = 512 × 512; in-plane resolution = 0.93 mm; slice thickness = 1 mm. Total imaging time was 1 h 57 min.

ROI delineation, quantitative analysis, and 3D reconstruction

ROIs were delineated by manual image segmentation (Fig. 2) of the MRI dataset using AMIRA software (FEI Visualization Sciences Group, Burlington, MA, USA). Segmentation was based on image grayscale intensity and a

priori knowledge of derived neural features characteristic of odontocete cetaceans (toothed whales, dolphins, and porpoises) and general mammalian neuroanatomy, spatial relationships, and external landmarks. Thresholding for signal intensity was used where possible; however, due to the large size of the specimen relative to the MR scanner bore, there was signal inhomogeneity across the tissue, rendering automatic segmentation ineffective. However, given the 1 mm isotropic resolution of the dataset, accurate parcellation of many complex structures was possible.

To accurately delineate gray and white matter within the total brain, cerebrum, brainstem, and cerebellum, exclusion of neurocranial adnexa such as the meninges, cerebral falx, cerebellar tentorium, cerebrospinal fluid (CSF), and retia mirabilia was undertaken. The final delineated cerebrum included the cortical gray matter (neocortex and allocortex) and cerebral white matter. Subcortical nuclei parcellated were the head of the caudate nuclei, composite structures of the putamina and globi pallidi, and thalamic nuclei. Basal ganglia nuclei that could not be reliably visualized and delineated were included with cerebral white matter. The delineated brainstem comprised both gray and white matter structures of the midbrain, pons, emergent cerebellar peduncles, and medulla oblongata anterior to the foramen magnum. The cerebellum was separated from the brainstem consistent with the guidelines described by Pierson et al. (2002). The final delineated cerebellum included the cerebellar hemispheres and vermis. Cerebellar nuclei could not be reliably parcellated and were consequently included with cerebellar white matter.

The corpus callosum was delineated through identification of anterior–posterior, dorsal-ventral, and lateral boundaries. The callosal sulcus and cingulate gyrus served as the anterior, dorsal, and ventral boundaries of the corpus callosum. The lateral ventricles and caudate nuclei formed the posterior boundary of the corpus callosum. In frontal view, the lateral extent of the corpus callosum was delimited by tracing a straight horizontal line from the posterior-most boundary of the cingulum to the ipsilateral lateral ventricle or caudate nucleus. This protocol permitted the delineation of the genu, truncus, and splenium of the corpus callosum while endeavoring to exclude the callosal radiations (forceps minor, tapetum, and forceps major) to surrounding white matter. Within the midline sagittal section, the outer contour of the corpus callosum was segmented.

The studies of *T. truncatus* neuroanatomy by Jacobs et al. (1979) and McFarland et al. (1969) aided identification of anatomical landmarks and hippocampal boundaries, and were essential to the development of the hippocampal segmentation protocol for the present study. Moreover, *Homo sapiens* hippocampal protocols (Morey et al. 2009; McHugh et al. 2007; Knoops et al. 2010) were adapted for
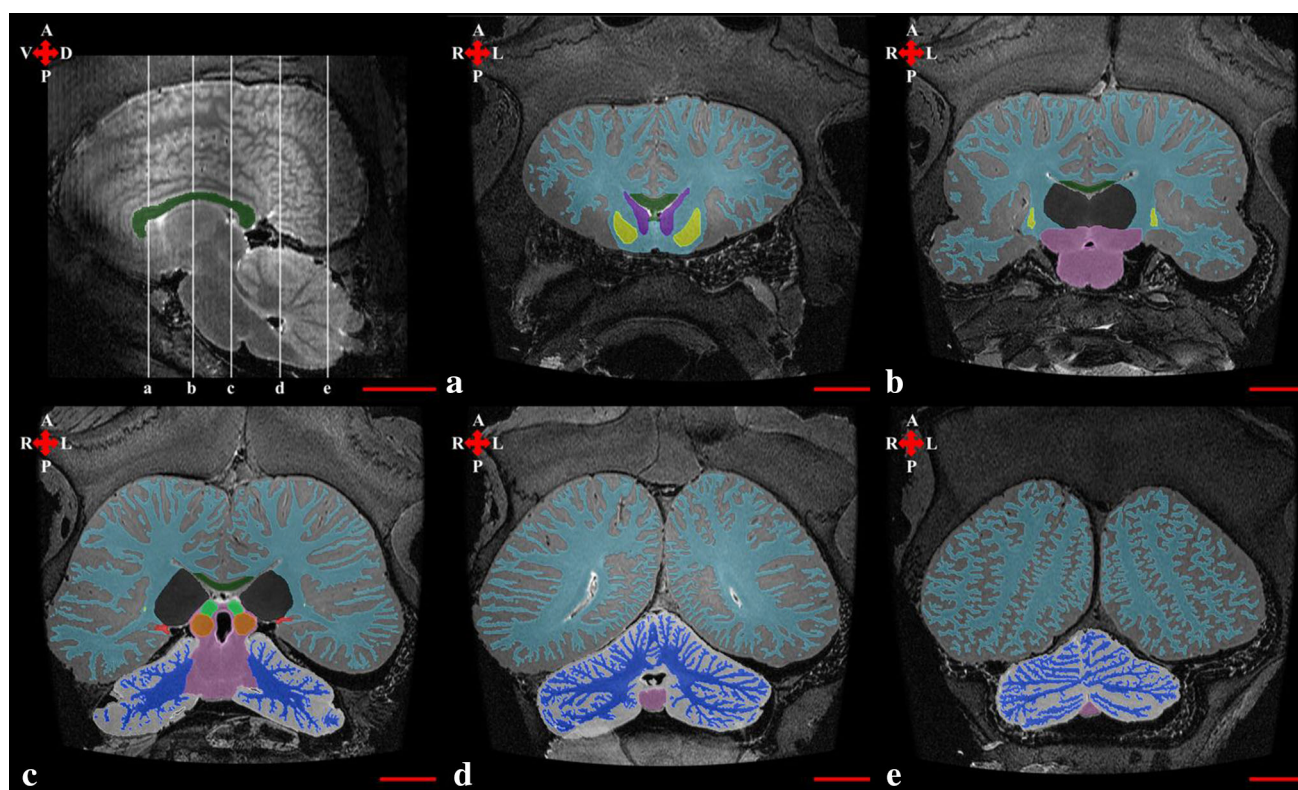
Fig. 2 Pilot parasagittal MR image and corresponding frontal MR images of the *O. orca* brain with representative manual parcellation of regions of interest (ROIs). *Parallel vertical lines* (*a–e*) on the parasagittal MR image represent the frontal planes of section. ROIs include cortical gray matter (*dark gray*), cerebral white matter (*light blue*), cerebellar gray matter (*light gray*), cerebellar white matter (*dark blue*), brainstem (*pink*), corpus callosum (*dark green*), hippocampi (*red*), superior colliculi (*light green*), inferior colliculi (*orange*), thalamic nuclei (*black*), putamina and globi pallidi (*yellow*), and caudate nuclei (*purple*). Anatomical directions: *A* (anterior), *P* (posterior), *D* (dorsal), *V* (ventral), *R* (right), and *L* (left). *Scale bar* ≈5 cm

O. orca hippocampus delineation. The ventral-anterior boundary of the hippocampus was demarcated by both the alveus, a thin white matter tract that separates the amygdala and hippocampus, and ventricular CSF. Continuing dorsally, CSF, choroid plexus, and the pulvinar thalami defined the anterior boundary of the hippocampus. The most dorsal boundary of the hippocampus was measured where the total length of the fornix was discernible. The white matter of the temporal lobe served as the posterior boundary of the hippocampus. Lateral and medial hippocampal boundaries were formed by the CSF of the lateral ventricles and subarachnoid space, respectively. The term hippocampus refers to a complex of subfields including the dentate gyrus, hippocampus proper, and subiculum. These hippocampal subfields were visually indistinguishable in this dataset and were consequently delineated as a singular complex and collectively designated as hippocampus.

The neuroendocrine structures of the pineal gland, anterior pituitary (adenohypophysis), and posterior pituitary (neurohypophysis) were also delineated.

Following image segmentation, ROI areas, volumes, and three-dimensional reconstructions were generated.

Neuroanatomical measurements included the total brain volume, total gray and white matter volumes, total cerebrum volume, cortical gray and cerebral white matter volumes, aggregate subcortical nuclei volume, caudate nuclei volume, putamina and globi pallidi volume, thalamic nuclei volume, total brainstem volume, total cerebellar volume, cerebellar gray and white matter volumes, corpus callosum volume and mid-sagittal area, hippocampal volumes, superior and inferior colliculi volumes and maximal cross-sectional areas, and neuroendocrine structure volumes. Total brain volume was multiplied by the specific gravity of brain tissue [1.036 g/cm^3; Gompertz 1902; Stephan 1960] to calculate brain mass. The percentage of the total brain occupied by a ROI was determined for each structure. The ratios of white matter volume relative to gray matter volume were derived for the total brain, cerebrum, and cerebellum. Callosal mid-sagittal area to calculated brain mass (CCA:BM), cortical gray matter volume to callosal mid-sagittal area, inferior colliculi volume to superior colliculi volume, and inferior colliculi cross-sectional area to superior colliculi cross-sectional area ratios were also calculated. To control for dimensional

inconsistency (Smith 2005), the ratios of the mid-sagittal corpus callosum area to the calculated brain mass (1) and the cortical gray matter volume to the callosal mid-sagittal area (2) were determined with the following equations:

$$\left\{\frac{\left[\sqrt{\text{callosal mid} - \text{sagittal area } (\text{cm}^2)}\right]}{\left[\sqrt[3]{\text{calculated brain mass (g)}}\right]}\right\} \quad (1)$$

$$\left\{\frac{\left[\sqrt[3]{\text{cortical gray matter volume } (\text{cm}^3)}\right]}{\left[\sqrt{\text{callosal mid} - \text{sagittal area } (\text{cm}^2)}\right]}\right\} \quad (2)$$

To determine scaling relationships between cortical gray matter, cerebral white matter, and cerebrum volumes in relation to total brain volume, bivariate reduced major axis (RMA) regression of $\log_{10}$-transformed volumetric data was performed with RMA for JAVA 1.21 (Bohonak and van der Linde 2004) to calculate scaling exponents (α). RMA regression was applied because both variables were subject to natural variation or measurement error, rendering ordinary linear regression inappropriate (Hofman et al. 1986). A t test was performed according to McArdle (1988) to test for the deviation of scaling exponents from isometry ($\alpha = \text{unity}$).

Annotated MR images

Annotated MR images of the *O. orca* brain are provided in Online Resource 1.

Results and discussion

Gray and white matter: total brain

The total brain volume for this *O. orca* was 6211.30 cm^3 (Table 1; Fig. 3). Total gray matter volume was 3676.74 cm^3 (Table 1; Fig. 3), while total white matter volume was 2374.88 cm^3 (excluding the neurohypophysis and brainstem gray and white matter structures; Table 1; Fig. 3). In this *O. orca*, the gray matter volume relative to total brain volume was 59.19 %, whereas relative white matter volume was 38.23 %, constituting nearly the remainder of brain volume. With 37.58 % of total brain volume occupied by white matter, the relative white matter extent of *L. acutus*, a small delphinid, is comparable to the much larger *O. orca* with a brain volume 5 times the size of that of *L. acutus* (Montie et al. 2008). In contrast, the proportion of total gray matter in *O. orca* is larger than that of *L. acutus* (55.47 %; Montie et al. 2008). Similar to *L. acutus*, the brain volume of *H. sapiens* is 5 times less than this *O. orca* with a relative gray matter volume of 55.38 % (data from Walhovd et al. 2011; Pakkenberg and

Gundersen 1997; Rilling and Insel 1999b). The amount of white matter relative to total brain size in *H. sapiens* is relatively large (42.65 %) compared to both *O. orca* and *L. acutus*. This finding suggests that the architecture of the delphinid brain emphasizes high local connectivity that minimizes conduction delay and increases computational power (Wen and Chklovskii 2005). This rapid processing power would appear to be necessary for the evolution of echolocation in delphinids such as *O. orca* and *L. acutus* living obligately within an aquatic environment that increases sound velocity.

Gray and white matter: cerebrum

The expansive cortical gray matter of this *O. orca* exhibited dramatic gyrification and sulcation, consistent with prior reports of cortical features in cetaceans (Ridgway and Brownson 1984; Hof et al. 2005; Manger et al. 2012). The cortical gray matter volume was 2999.52 cm^3 (Table 1; Figs. 3, 4), comprising nearly 50 % of the total brain volume. The volumes of the cerebral white matter (Table 1; Fig. 3), aggregate subcortical nuclei (Table 1; Fig. 4), and neuroendocrine structures (Table 1; Figs. 3, 5) expressed as percentages of total brain volume were 33.26, 2.08, and 0.04 %, respectively. The pineal gland (Fig. 5), while previously elusive in other cetacean species (for review, Panin et al. 2012), was presumably identified in this *O. orca*; however, histological evaluation is required for confirmation, but was not possible for the present study due to alteration of the specimen following MRI.

The cerebrum (cortical gray matter and cerebral white matter, excluding the hippocampus) of *O. orca* constitutes 81.51 % of the total brain volume (Table 2). The profound corticalization of this *O. orca* (Fig. 3) may only be exceeded by the sperm whale (*Physeter macrocephalus*; Ridgway and Hanson 2014), the largest odontocete cetacean, and is unsurpassed compared to other mammalian taxa (Table 2; Clark et al. 2001), including *H. sapiens* for which the cerebrum occupies 76.18 % of the total brain volume (Table 2; data from Walhovd et al. 2011; Pakkenberg and Gundersen 1997; Rilling and Insel 1999b). These results are consistent with previous research concerning *O. orca* cortical surface area (Ridgway and Brownson 1984). Voluminous cerebra are characteristic of delphinoid cetaceans with relative sizes ranging from 70.39 to 73.40 % of total brain size (Table 2) in five species (*P. phocoena*, *T. truncatus*, *Globicephala macrorhynchus*, *Grampus griseus*, and *S. coeruleoalba*) of varying brain size (Haug 1970; Hofman 1985, 1988). Mammalian cortical enlargement has been associated with prolonged maternal investment (Barton and Capellini 2011) and developmental period (Joffe 1997), sociality (Dunbar 1998; Shultz and Dunbar 2006), and sensory specialization

Table 1 Measurements of neural regions of interest (ROIs) for *O. orca* and literature review of neuroanatomical data available for odontocete cetaceans

ROI measurement	Wright et al.	Literature review	
	O. orca	*O. orca*[a]	Odontoceti[a,b]
Brain mass (g)	–	(4500.00–9300.00)[1,2]	(205.00–9200.00)[1,2,3,4,5,6,7]
Calculated brain mass (g)[c]	6434.91	–	–
Brain volume (cm³)	6211.30	–	(483.00–3650.00)[7,8,9,10,11]
WM[d]	2374.88	–	(467.04–475.83)[7]
GM[e]	3676.74	–	(673.31–718.55)[7]
WM:GM[f]	0.65	–	(0.66–0.71)[7]
Cerebrum volume (cm³)	5065.55	–	(340.00–2045.00)[8,9,10]
Cerebral WM[d]	2066.03	–	(135.00–868.00)[8,9,10]
Cortical GM[e,g]	2999.52	–	(205.00–1177.00)[8,9,10]
WM:GM[f]	0.69	–	(0.66–0.81)[8,9,10]
% of brain[h]	81.55	–	(70.39–73.40)[8,9,10]
Subcortical nuclei volume (cm³)	129.14	–	–
% of brain[h]	2.08	–	–
Caudate nuclei	10.19	–	–
Globi pallidi + putamina	14.09	–	–
Thalamic nuclei	104.86	–	(18.00–52.50)[8]
Neuroendocrine volume (cm³)	2.65	–	–
% of brain[h]	0.04	–	–
Adenohypophysis	2.20	–	(0.17–1.50)[4,12,13,14,15,16]
Neurohypophysis	0.25	–	(0.21)[12]
Pineal gland	0.20	–	–
Brainstem volume (cm³)	157.02	–	(21.00–209.00)[8]
% of brain[h]	2.53	–	(4.35–6.83)[8]
Cerebellum volume (cm³)	856.93	(727.00–1544.00)[2]	(92.66–656.00)[2,7,11]
WM[d]	308.85	–	(53.17–61.71)[7]
GM[e]	548.08	–	(110.42–113.67)[7]
WM:GM[f]	0.56	–	(0.47–0.56)[7]
% of brain[h]	13.80	(11.80–17.20)[2]	(5.00–18.20)[2,4,7,11]
Corpus callosum volume (cm³)	27.19	–	–
% of brain[h]	0.44	–	–
Corpus callosum mid-sagittal area (cm²)	4.29	(4.47–8.29)[17,18]	(1.04–4.63)[7,17,18]
CCA:BM[i]	0.11	(0.12–0.15)[17,18]	(0.11–0.17)[7,17,18]
Cortical GM:CCA[j]	6.96	–	(4.71–5.87)[10,17,18]
Hippocampus volume (cm³)	2.46	–	(0.60–1.90)[7,19]
% of brain[h]	0.04	–	(0.07–0.15)[7,19]
Left	1.10	–	(0.87–1.04)[7]
Right	1.35	–	(0.74–0.86)[7]
Superior colliculus volume (cm³)	2.40	–	–
% of brain[h]	0.04	–	–
Left	1.11	–	–
Right	1.29	–	–
Superior colliculus maximal cross-sectional area (mm²)[k]	235.52	–	(6.00–118.80)[1,4,20]
Left	108.42	–	–
Right	127.11	–	–

Table 1 continued

ROI measurement	Wright et al.	Literature review	
Inferior colliculus volume (cm^3)	6.07	–	–
% of brain[h]	0.10	–	–
Left	2.94	–	–
Right	3.13	–	–
Inferior colliculus maximal cross-sectional area (mm^2)[k]	530.86	–	(75.40–296.10)[1,4,20,21]
Left	246.27	–	–
Right	284.59	–	–
IC volume:SC volume[l]	2.53	–	–
IC cross-sectional area:SC cross-sectional area[m]	2.25	–	(2.20–28.30)[1,4,20]

[a] Range of ROI measurement from data in cited literature; [b] excluding *O. orca*; [c] calculated brain mass (g) = brain volume (cm^3) × brain tissue specific gravity [1.036 g/cm^3; Gompertz (1902); Stephan (1960)]; [d] *WM* white matter; [e] *GM* gray matter; [f] WM:GM = white matter volume (cm^3)/gray matter volume (cm^3); [g] including hippocampus; [h] percentage of total brain comprised by ROI; [i] CCA:BM = [corpus callosum mid-sagittal area (cm^2)]$^{1/2}$/[calculated brain mass (g)]$^{1/3}$; [j] Cortical GM:CCA = [cortical gray matter volume (cm^3)]$^{1/3}$/[corpus callosum mid-sagittal area (cm^2)]$^{1/2}$; [k] collicular cross-sectional area (mm^2) = [length (mm) × width (mm) × π]/4; [l] IC volume:SC volume = inferior colliculi volume (cm^3)/superior colliculi volume (cm^3); [m] IC cross-sectional area:SC cross-sectional area = inferior colliculi cross-sectional area (mm^2)/superior colliculi cross-sectional area (mm^2)

[1] Pilleri and Gihr (1970); [2] Ridgway and Hanson (2014); [3] Jacobs and Jensen (1964); [4] Pilleri (1972); [5] Ridgway and Brownson (1984); [6] Ridgway and Tarpley (1996); [7] Montie et al (2008); [8] Haug (1970); [9] Hofman (1985); [10] Hofman (1988); [11] Marino et al. (2000); [12] Wislocki (1929); [13] Gihr and Pilleri (1969); [14] Pilleri and Gihr (1969); [15] Gruenberger (1970); [16] Pilleri and Gihr (1972); [17] Tarpley and Ridgway (1994); [18] Keogh and Ridgway (2008); [19] Patzke et al. (2013); [20] Chen (1979); [21] Oelschläger et al. (2010)

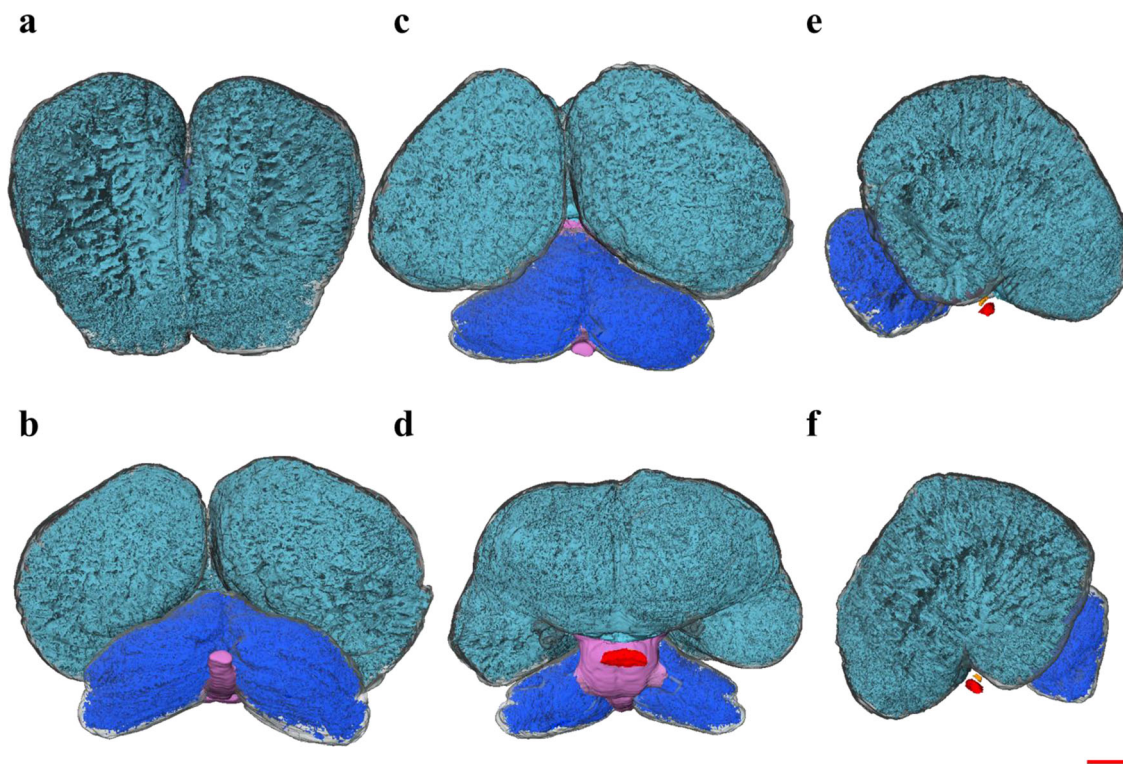**Fig. 3** **a** Anterior, **b** posterior, **c** dorsal, **d** ventral, **e** right parasagittal, and **f** left parasagittal views of the *O. orca* brain segmented into cortical gray matter (*translucent dark gray*), cerebral white matter (*light blue*), adenohypophysis (*red*), neurohypophysis (*orange*), brainstem (*pink*), cerebellar gray matter (*translucent light gray*), and cerebellar white matter (*dark blue*). *Scale bar* ≈ 5 cm
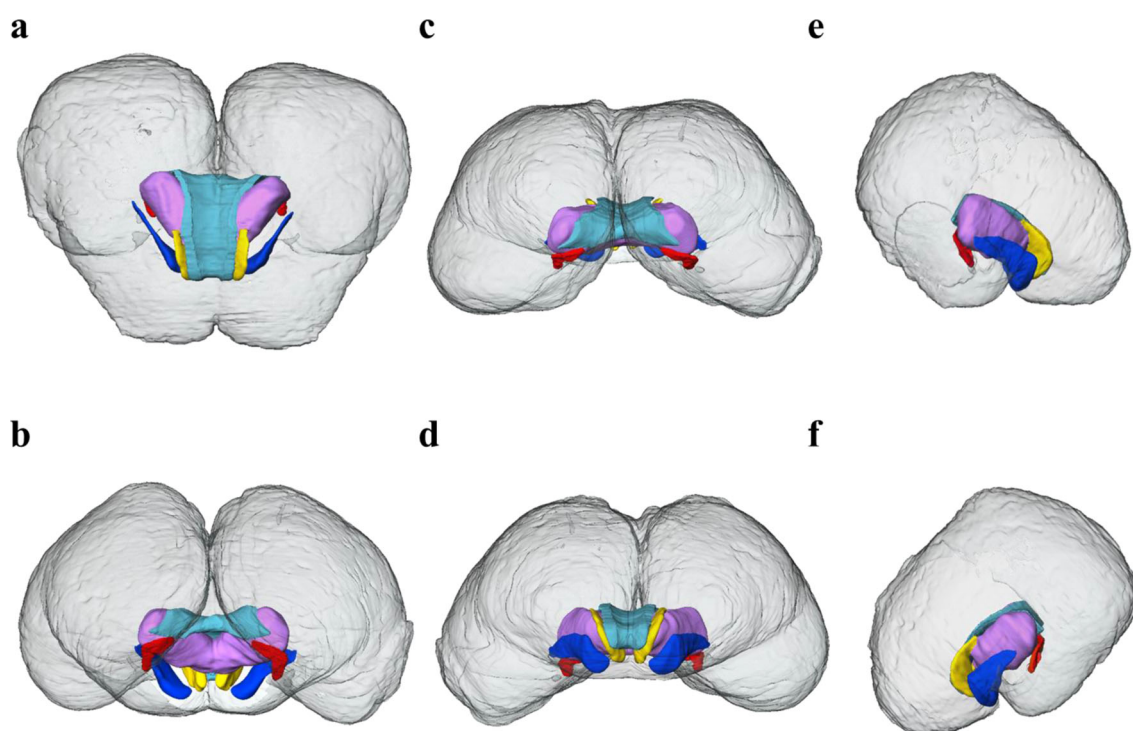
Fig. 4 **a** Anterior, **b** posterior, **c** dorsal, **d** ventral, **e** right parasagittal, and **f** left parasagittal views of the *O. orca* cerebrum segmented into cortical gray matter (*translucent dark gray*), corpus callosum (*light blue*), hippocampi (*red*), caudate nuclei (*yellow*), putamina and globi pallidi (*dark blue*), and thalamic nuclei (*purple*). *Scale bar* ≈ 5 cm

(Barton 1998, 2006) which are traits common to delphinoids, and the wider Odontoceti. Moreover, cortical size has been suggested as a good predictor of cognitive ability (Reader and Laland 2002; Byrne and Bates 2007). However, recent studies propose that absolute neuron number, irrespective of body size, may be a better determinant of cognitive performance (Herculano-Houzel 2011; Roth and Dicke 2005). A limited number of studies using unbiased stereological methods have estimated the total cortical neuron number of cetaceans. *P. phocoena* and *Globicephala melas* both have high numbers of cortical neurons; moreover, *G. melas* has almost twice as many neurons as *H. sapiens* (Mortensen et al. 2014; Walløe et al. 2010). Considering the corpus of research on the cognitive abilities of delphinoid cetaceans (for review, Herman 2010; Würsig 2009, but cf. Manger 2013), it will be of great interest to determine the absolute neuron number of the highly corticalized *O. orca*, thus offering an opportunity to explore the intersection of delphinoid brain and cognitive evolution.

A distinctive feature of delphinoid brain evolution is the deviation from allometric scaling relationships between cortical gray and white matter volumes that are otherwise evolutionarily conserved. Typical mammalian brain allometry exhibits hyperscaling of cortical white matter

with increasing brain size (Barton and Harvey 2000; Zhang and Sejnowski 2000). It has been proposed that larger brains require thicker, more abundant, and heavily-myelinated long-range axonal connections between different brain regions to minimize conduction delay, resulting in a disproportionate expansion of cortical white matter (Wen and Chklovskii 2005; Zhang and Sejnowski 2000; Changizi 2001). Curiously, the cerebral white matter of *O. orca*, with possibly the largest brain in the animal kingdom (Ridgway and Hanson 2014), and of the delphinoids examined (data from Haug 1970; Hofman 1988) scales isometrically with total brain volume, rendering a scaling exponent of $\alpha = 1.059$ [t test, degrees of freedom (df) = 3, $P = 0.88$] and extending previous findings by Hofman (1989). Furthermore, overall cerebral volume (cortical gray matter and cerebral white matter) and cortical gray matter volume did not depart from isometry [($\alpha = 1.045$, t test, $df = 4$, $P = 0.85$ and $\alpha = 1.05$, t test, $df = 3$, $P = 0.71$, respectively; data from Haug 1970; Hofman 1985, 1988]. In other words, cortical proportionality is relatively fixed across delphinoid species thus far examined with the proportion of cortical gray matter and cerebral white matter minimally altered with brain enlargement. As a consequence, despite a nearly 13-fold difference in brain size between *O. orca* and *P. phocoena*, relative cortical gray matter and cerebral
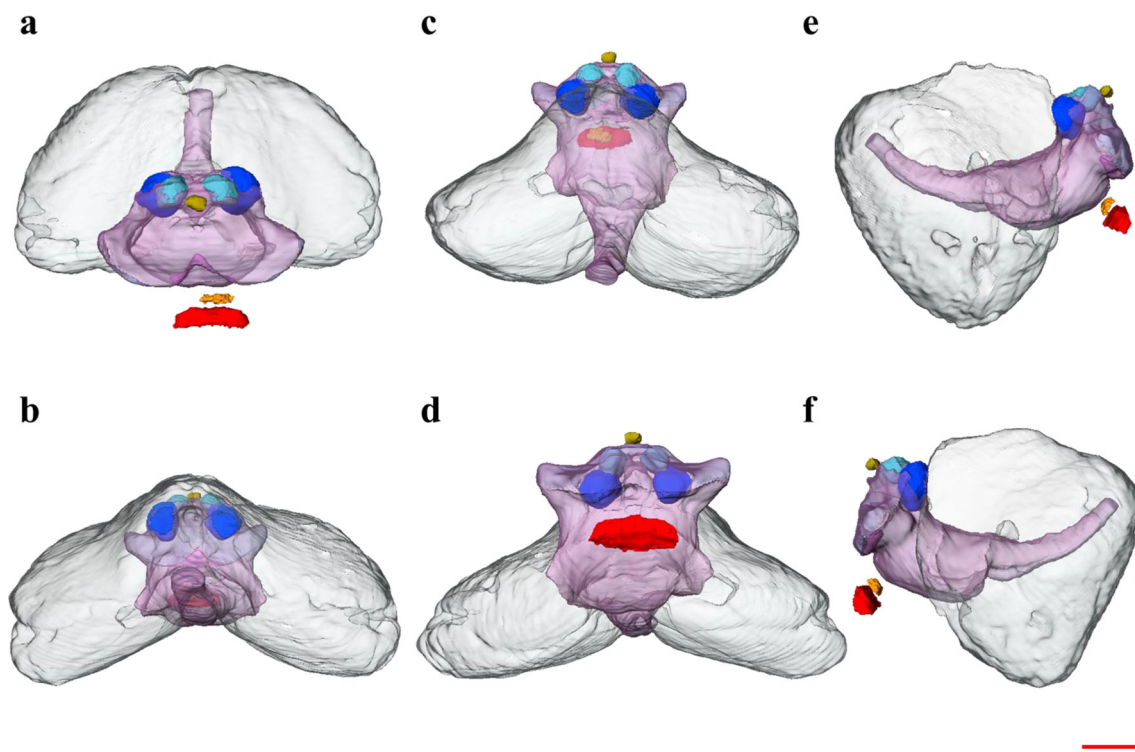
Fig. 5 **a** Anterior, **b** posterior, **c** dorsal, **d** ventral, **e** right parasagittal, and **f** left parasagittal views of the *O. orca* adenohypophysis (*red*), neurohypophysis (*orange*), pineal gland (*gold*), brainstem (*translucent pink*), superior colliculi (*light blue*), inferior colliculi (*dark blue*), and cerebellar gray matter (*translucent light gray*). *Scale bar* ≈3 cm

Table 2 Brain, cerebrum (cortical GM and cerebral WM), cortical GM, and cerebral WM volumes and percentage of total brain occupied by these volumes in *O. orca* and other mammals

	Brain (cm³)	Cerebrum (cm³)[a]	Cortical GM (cm³)[a,b]	Cerebral WM (cm³)[c]	% Cerebrum	% Cortical GM	% Cerebral WM
O. orca	6211.30	5063.10	2997.07	2066.03	81.51	48.25	33.26
Delphinoid cetaceans[d,1,2,3]	483.00–2786.00	340.00–2045.00	205.00–1177.00	135.00–868.00	70.39–73.40	39.29–42.44	27.95–31.68
Artiodactyls[3,4,5]	105.00–486.00	71.60–337.00	51.80–226.00	19.80–111.00	60.22–69.34	46.50–49.33	18.86–22.84
Sirenians[6,7]	223.00–439.19	127.46–283.01	–	–	57.16–67.25	–	–
Proboscideans[2,8]	3886.70–4148.00	2460.10–2491.00	1378.70–1402.00	1081.40–1089.00	60.05–63.30	33.80–35.47	26.25–27.82
Anthropoid primates[9,10,11]	23.10–1225.38	16.50–933.54	11.70–506.88	4.80–426.66	62.14–76.18	38.43–50.65	19.70–34.82

[a] Excluding hippocampus volume; [b] *GM* gray matter; [c] *WM* white matter; [d] excluding *O. orca*

[1] Haug (1970); [2] Hofman (1985); [3] Hofman (1988); [4] Schlenska (1974); [5] Meyer (1981); [6] Pirlot and Kamiya (1985); [7] Reep and O'Shea (1990); [8] Hakeem et al. 2005; [9] Pakkenberg and Gundersen (1997); [10] Rilling and Insel (1999b); [11] Walhovd et al. (2011)

white matter volumes exhibit limited ranges of 39.29–48.25 and 27.95–33.26 %, respectively, across delphinoids (Table 2). Further cross-species studies are needed to determine whether isometric scaling of cerebral tissues is a trait that is widespread within, or unique to, the Delphinoidea, or that characterizes the wider Odontoceti or Mysticeti (baleen whales), more generally. Studies demonstrating callosal isometry in a range of cetacean species (Gilissen 2006; Manger et al. 2010) tentatively suggest that the isometric cerebral scaling observed in the delphinoids studied to date may be a defining neuroanatomical feature of Cetacea.

The absence of cerebral white matter hyperscaling in delphinoid cetaceans suggests that conduction velocity is either compromised or optimized by alternative mechanisms. Studies of auditory brainstem response in delphinids measured latencies that were shorter than predicted on the basis of brain size, indicating a higher conduction velocity

compared to other mammals (Ridgway et al. 1981). Conduction velocity along mammalian myelinated axons increases with axon diameter (Hursh 1939), degree of myelination (Waxman 1980), and neuron-glia interactions (Yamazaki et al. 2007). The cranial nerves of delphinoid cetaceans have the largest axon diameters reported for all mammals (Gao and Zhou 1991, 1992; Dawson et al. 1982). The cochlear nerve of *Neophocaena phocaenoides*, the finless porpoise, contains giant axons as thick as 54.9 μm (Gao and Zhou 1991). The significant proportion of giant axons within the cochlear nerve indicates specialization for rapid transmission of acoustic stimuli in delphinoids (Gao and Zhou 1992). While delphinoid cranial nerves contain the highest percentages of large-diameter axons compared to other mammals, they exhibit the lowest axonal densities (Gao and Zhou 1992). The low axonal densities observed across delphinoid species may account for the absence of white matter hyperscaling in these taxa. Moreover, low axonal density suggests a relatively high proportion of neuroglia—astrocytes, oligodendrocytes, NG2-glia, and microglia—within white matter (Herculano-Houzel 2014). Though glial subpopulations have not yet been quantified in cetaceans, one study identified high astroglial content within the optic nerves of *S. coeruleoalba* (suborder Odontoceti) and *Balaenoptera physalus* (suborder Mysticeti; Mazzatenta et al. 2001). Oligodendrocytes support neuronal function by producing axon-ensheathing myelin that allows for faster signal propagation (Verkhratsky and Butt 2013). Furthermore, depolarization of oligodendrocytes has been demonstrated to directly increase the conduction velocity of action potentials (Yamazaki et al. 2007). Thus, conduction velocity could be optimized in delphinoids through amplifying interactions between axons and ancillary oligodendrocytes. Axonal gigantism, low axonal densities, and potentially high numbers of white matter glial cells per axon in the large brains of delphinoid cetaceans indicate that different mechanisms to white matter hyperscaling evolved to support rapid information processing across greater transmission distances in this taxon.

The evolutionary process of adaptation to an obligatory aquatic existence dramatically modified cetacean brain morphology and function. Isometric scaling of cerebral tissues with brain volume may have arisen due to rigid constraints imposed by the marine environment on delphinoids. Indeed, interhemispheric connectivity (Gilissen 2006; Manger et al. 2010), cortical surface area (Ridgway and Brownson 1984) and gyrencephaly (Manger et al. 2012) also scale isometrically in the Odontoceti. Moreover, odontocete middle ear bones exhibit isometric scaling indicating that these echolocating mammals were under considerable selective pressure for the preservation of certain auditory structure dimensions (Nummela et al.

1999) that conceivably enhanced underwater hearing ability. Considering the unique cerebral isometry of delphinoids, it may be suggested that significant advantages were gained from the restriction of cerebral white matter hyperscaling. The volume of cortical gray matter expressed as a percentage of cerebral volume was 59.19 % for this *O. orca* and averaged 57.84 % across delphinoids (data from Haug 1970; Hofman 1988), comprising the majority of cerebral space. Within the cerebrum of delphinoid cetaceans, the proportion of cortical gray matter appears to be larger than that of *H. sapiens* (54.30 %; data from Walhovd et al. 2011; Pakkenberg and Gundersen 1997; Rilling and Insel 1999b) and the African elephant (*Loxodonta africana*; 56.16 %; data from Hofman 1985; Hakeem et al. 2005), a mammal with the largest brain among extant and extinct terrestrial mammals. Conversely, the volume of cerebral white matter relative to the total cerebrum averaged 42.16 % across the delphinoids examined, compared to 45.70 % in *H. sapiens* (data from Walhovd et al. 2011; Pakkenberg and Gundersen 1997; Rilling and Insel 1999b) and 43.84 % in *L. africana* (Hofman 1985; Hakeem et al. 2005). Delphinoids may have evolved this divergent cortical morphology in response to the sensorimotor demands of the aquatic environment. Cortical gray matter contains networks of neurons that in large brains exhibit dense clustering, high local connectivity, and sparse global connectivity, resembling a 'small-world' network (Bassett and Bullmore 2006; Watts and Strogatz 1998). These 'small-world' properties are thought to play a central role in cortical information processing by minimizing conduction delay and enhancing computational power (Wen and Chklovskii 2005). Thus, in the aquatic environment, where sound velocity is accelerated compared to air, increased local connectivity (gray matter) at the expense of global connectivity (white matter) in the cerebrum of delphinoid cetaceans could potentially support rapid auditory analysis and reduce motor response latencies to acoustic stimuli. Selection for high local connectivity and short conduction delay in the delphinoid cortex is suggested by increased cortical gray matter volume, unparalleled gyrencephaly (Manger et al. 2012; Hofman 2012), unique cortical topography (Ladygina et al. 1978), commissural deficit (Tarpley and Ridgway 1994), hemispheric asymmetry (Ridgway and Brownson 1984), and functional lateralization (MacNeilage 2013; Ringo 1991).

Though delphinoid cortical gray matter is expansive and contains large numbers of neurons, neuronal density is low resulting in increased numbers of glial cells per neuron (Mortensen et al. 2014; Walløe et al. 2010; Herculano-Houzel 2014). The cortical glial cell to cortical neuron ratios of *G. melas* and *P. phocoena* are higher than that in *H. sapiens* (1.4:1) at 3.4:1 and 2.3:1, respectively (Pakkenberg and Gundersen 1997; Mortensen et al. 2014;

Walløe et al. 2010). Moreover, *Balaenoptera acutorostrata*, the minke whale, has one of the highest ratios of cortical glial cells to cortical neurons (7.7:1) studied to date (Eriksen and Pakkenberg 2007). An increased number of glial cells per neuron may be advantageous for species inhabiting the aquatic environment by enhancing neuronal signaling and conferring neuroprotective benefits; however, an alternative hypothesis on the potential thermogenetic function of cetacean glia has been proposed previously (Manger 2006), albeit controversial and as yet unsupported quantitatively (Marino et al. 2008; Maximino 2009a, b). High numbers of astrocytes and oligodendrocytes could potentially support rapid processing of acoustic information by regulating synaptogenesis (Ullian et al. 2001), enhancing synaptic efficacy (Pfrieger and Barres 1997), and increasing conduction velocity (Yamazaki et al. 2007). Astrocytes are relatively resistant to hypoxic conditions (Swanson et al. 1997), and afford neuroprotective benefits to adjacent neurons that are more vulnerable to hypoxic insult. During hypoxia, astrocytes can augment glycolytic capacity (Marrif and Juurlink 1999), downregulate synaptic activity (Martín et al. 2007), and upregulate erythropoietin to potentially inhibit hypoxia-induced apoptosis (Ruscher et al. 2002). Thus, astrocyte-mediated neuroprotection may serve a critical role for cetaceans which spend the majority of their time underwater and are reliant on limited oxygen stores at depth. Moreover, higher glial content per neuron may have permitted the ancestors of extant cetaceans to successfully invade the aquatic environment by enhancing hypoxia tolerance and limiting conduction delay. In support of this hypothesis, a recent study of cellular composition within the cerebral cortex of artiodactyls, the closest phylogenetic relatives of cetaceans (Gatesy et al. 2013), found high numbers of non-neuronal (presumably mostly glial) cells per neuron (Kazu et al. 2014). High non-neuronal cell to neuron ratios have also been measured in *L. africana* (Herculano-Houzel et al. 2014), one of the closest phylogenetic relatives to obligately aquatic sirenians (dugongs and manatees; Seiffert 2007), suggesting that increased numbers of glial cells per neuron may have been necessary to facilitate the evolutionary transition from terrestrial to obligatory aquatic existence.

Gray and white matter: brainstem

The brainstem of this *O. orca* occupied 2.53 % of the total brain volume at 157.02 cm^3 (Table 1; Figs. 3, 5). The relative volume of the brainstem in this *O. orca* compared to other delphinoids is considerably small. The relative size of the brainstem in *P. phocoena, T. truncatus, and G. macrorhynchus* is 4.35, 4.38, and 6.83 %, respectively (Haug 1970). The divergence in relative brainstem volumes

across these species may reflect the greater corticalization of *O. orca* in comparison to other delphinoids. These discrepant measurements may also arise from sampling error, dissimilar methodology, or differential shrinkage of heterogeneous brain tissues in fixative (Kretschmann et al. 1982; Quester and Schröder 1997). The relative volume of the brainstem in *O. orca* is larger than that of *H. sapiens* (1.97 %; Walhovd et al. 2011). This increased relative size may be ascribed to hypertrophy of various components of the auditory, trigeminal, and motor systems (for review, Oelschläger 2008).

Gray and white matter: cerebellum

The cerebellum of *O. orca* was voluminous, constituting 13.80 % of the total brain size. Total cerebellar volume was 856.93 cm^3 (Table 1; Figs. 3, 5), consisting of gray and white matter volumes that were 548.08 and 308.85 cm^3, respectively (Table 1). The large cerebellum in *O. orca* is consistent with previous measurements of cerebellar size in *O. orca* (Ridgway and Hanson 2014), and other odontocete cetaceans (Montie et al. 2008; Ridgway and Tarpley 1996; Marino et al. 2000; Pilleri 1972). The large cerebella relative to total brain size observed in delphinoid cetaceans may signal an integral role for the cerebellum in acoustic processing and potentially higher-order cognitive functions such as learning and memory. The paraflocculus, an auditory-associated cerebellar region, is particularly expanded in odontocetes and echolocating bats (Hanson et al. 2013; Larsell 1970) and may be vital for acousticomotor processing related to sound production and navigation (Oelschläger 2008). Moreover, anatomical and functional MRI studies have implicated the paraflocculus in verbal working memory (lobules VIIIa, VIIIb, and IX; Cooper et al. 2012) and episodic memory retrieval (lobule IX; Habas et al. 2009).

Corpus callosum

The volume of this *O. orca* corpus callosum was 27.19 cm^3 occupying 0.44 % of the total brain volume and 1.32 % of cerebral white matter volume (Table 1; Fig. 4). The small volume of the *O. orca* corpus callosum is consistent with previous measurements of callosal extent in other odontocete species (Montie et al. 2008; Tarpley and Ridgway 1994; Keogh and Ridgway 2008). The mid-sagittal corpus callosum area of this *O. orca* was 4.29 cm^2 (Tables 1, 3). The ratio of the square root of the corpus callosum mid-sagittal area (cm^2) to the cube root of the calculated brain mass (g) [CCA:BM] was 0.11 (Tables 1, 3), illustrating the diminutive size of the *O. orca* corpus callosum relative to brain mass. Although this value fell below the range of CCA:BM ratios (0.12–0.15) calculated from previously

Table 3 Brain mass (BM), callosal mid-sagittal area (CCA), CCA:BM, and cortical GM:CCA in *O. orca* and other mammals

	BM (g)	CCA (cm^2)	CCA:BM[a]	Cortical GM:CCA[b]
O. orca[1]	6434.91	4.29	0.11	6.96
O. orca[c,2,3]	5667.00–7100.00	4.47–8.29	0.12–0.15	–
Odontocete cetaceans[d,2,3,4,5]	514.00–4739.00	1.04–4.63	0.11–0.17	4.71–5.87
Artiodactyls[6,7,8]	244.00–530.00	1.17–1.93	0.16–0.22	–
Sirenians[2,6,7]	188.00–302.00	0.90–2.50	0.17–0.24	–
Proboscideans[6,7,9,10]	4026.62–5250.00	8.09–12.57	0.17–0.22	3.11
Pinnipeds[2,6,7]	345.00–1250.00	1.01–1.89	0.13–0.17	–
Anthropoid primates[11,12,13]	23.93–1345.66	0.44–6.90	0.21–0.24	3.16–3.61

[a] CCA:BM = [corpus callosum mid-sagittal area (cm^2)]$^{1/2}$/[calculated brain mass (g)]$^{1/3}$; [b] Cortical GM:CCA = [cortical gray matter volume (cm^3)]$^{1/3}$/[corpus callosum mid-sagittal area (cm^2)]$^{1/2}$; [c] excluding *O. orca* data from Wright et al; [d] excluding *O. orca*

[1] Wright et al.; [2] Tarpley and Ridgway (1994); [3] Keogh and Ridgway (2008); [4] Hofman (1988); [5] Montie et al. (2008); [6] Anthony (1938); [7] Manger et al. (2010); [8] Butti et al. (2014b); [9] Hakeem et al. (2005); [10] Shoshani et al. (2006); [11] Rilling and Insel (1999a); [12] Rilling and Insel (1999b); [13] Fears et al (2009)

reported callosal data for *O. orca* (Tables 1, 3; Tarpley and Ridgway 1994; Keogh and Ridgway 2008), it lies within the range of CCA:BM ratios (0.11–0.17) calculated for wider Odontoceti (Tables 1, 3; Montie et al. 2008; Tarpley and Ridgway 1994; Keogh and Ridgway 2008). The slight departure of this specimen from the CCA:BM ratio range established for *O. orca* (Tarpley and Ridgway 1994; Keogh and Ridgway 2008) may reflect discrepancies in measurement arising from comparison of fresh versus fixed tissues (shrinkage artifact; Schulz et al. 2011), or alternatively, sampling error or divergent methodology. Despite these comparative limitations, it is apparent that this *O. orca* along with conspecifics and wider Odontoceti, exhibit lower interhemispheric connectivity compared to most other mammals, except for the semi-aquatic Pinnipedia (seals, sea lions, and walruses; Table 3; Manger et al. 2010).

The ratio of the cube root of cortical gray matter volume (cm^3) to the square root of callosal mid-sagittal area (cm^2) in *O. orca* (6.96; Tables 1, 3) was larger than the ratios for the delphinids, *G. griseus* (5.87), *G. macrorhynchus* (5.21), and *T. truncatus* (4.71; delphinid data from Haug 1970; Hofman 1988; Tarpley and Ridgway 1994; Keogh and Ridgway 2008), as well as the large-brained terrestrial mammals, *H. sapiens* (3.18; Rilling & Insel 1999a) and *L. africana* (3.11; Hakeem et al. 2005). Thus, the callosal area per unit volume of cortical gray matter in other delphinids, *H. sapiens*, and *L. africana* was 1.32, 2.19, and 2.24 times larger than that of this *O. orca*.

As the major commissural linkage between the cerebral hemispheres, the relatively small callosal size of *O. orca* and other odontocete cetaceans presumably supports greater hemispheric independence than in other mammalian orders (Ridgway 1990). Indeed, odontocete unihemispheric slow wave sleep (USWS), a state of interhemispheric asymmetry in which one cerebral hemisphere produces sleeping electroencephalograms (EEGs) while the opposite hemisphere produces waking EEGs (for review, Lyamin et al. 2008), is likely associated with reduced interhemispheric communication via the small corpus callosum. USWS is proposed to support locomotion required for surface respiration as well as environmental monitoring for detection of conspecifics, predators, and prey (Lyamin et al. 2008; Goley 1999; Rattenborg et al. 2000). Additionally, USWS facilitated by reduced callosal linkage, may also limit cerebral O$_2$ metabolism through unihemispheric vasoconstriction and reduction in cerebral blood flow and glucose consumption (Ridgway et al. 2006).

Hippocampus

The hippocampus is a limbic structure subserving learning, memory, and spatial navigation (Burgess et al. 2002). The cetacean hippocampus is widely recognized as diminutive, both in absolute size and relative to the size of the brain as a whole (Table 4; Morgane et al. 1982; Jacobs et al. 1979; Patzke et al. 2013). The hippocampi of *O. orca* are no exception, with hippocampal volume measuring 2.46 cm^3, constituting 0.04 % of the total brain volume (Tables 1, 4; Fig. 4). The left and right hippocampi of *O. orca* were 1.10 and 1.35 cm^3 (Table 1), respectively, exhibiting an asymmetry of hippocampal size similar to that observed in *L. acutus* (Montie et al. 2008). The percentage of the total brain occupied by the hippocampus in cetaceans varies from 0.04 to 0.15 % (Table 4), with *O. orca* representing the lower boundary of the range. The relative hippocampal volumes of cetaceans are the smallest of all mammals examined (Table 4). Interestingly, the relative hippocampal volume of the large-brained *L. africana* (0.21–0.23 %; data from Patzke et al. 2013) more closely approaches this measure in cetaceans than do the relative hippocampal

Table 4 Brain and hippocampal volumes and percentage of total brain occupied by the hippocampus in *O. orca* and other mammals

	Brain volume (cm^3)	Hippocampal volume (cm^3)	% Hippocampus
O. orca	6211.30	2.46	0.04
Cetaceans[a,1,2]	469.11–2799.23	0.60–1.90	0.05–0.15
Artiodactyls[2,3,4]	77.70–559.27	2.67–8.58	0.92–3.44
Sirenians[2,3,5]	223.00–337.84	2.07–3.63	0.93–1.07
Proboscideans[2]	4666.99–5067.57	10.57–11.21	0.21–0.23
Pinnipeds[2,3]	265.44–638.27	1.95–3.53	0.55–0.79
Anthropoid primates[6]	4.34–1283.78	0.13–10.29	0.80–3.27

[a] Excluding *O. orca*

[1] Montie et al. (2008); [2] Patzke et al. (2013); [3] Reep et al. (2007); [4] Butti et al. (2014b); [5] Pirlot and Kamiya (1985); [6] Stephan (1981)

volumes of obligatorily aquatic sirenians (0.93–1.07 %; data from Patzke et al. 2013; Reep et al. 2007; Pirlot and Kamiya 1985), or semi-aquatic pinnipeds (0.55–0.79 %; data from Patzke et al. 2013; Reep et al. 2007).

The poor development of the cetacean hippocampus compared to other mammals (Table 4; Patzke et al. 2013) and its apparent lack of adult neurogenesis (Patzke et al. 2013) is enigmatic, given the high cognitive function (for review, Herman 2010; Würsig 2009; but cf. Manger 2013) and navigational prowess (Block et al. 2011; Durban and Pitman 2012) observed in Cetacea. Patzke et al. (2013) proposed that the unusual cetacean hippocampal morphology and apparent absence of hippocampal neurogenesis may be related to their mammalian-atypical sleep physiology [i.e., limited or potentially absent rapid eye movement (REM) sleep; for review, Lyamin et al. 2008]. However, the presence of well-developed hippocampi and hippocampal neurogenesis in obligatorily aquatic sirenians and semi-aquatic pinnipeds (Patzke et al. 2013) along with observations of reduced REM sleep in these taxa (for review, Lyamin et al. 2008) would not seem to support this hypothesis. Therefore, it is posited that the small size of the cetacean hippocampus may arise from a suite of phenomena related to sensory function, rather than sleep physiology.

The dominant sensory mode of odontocete cetaceans is echolocation, a high resolution sensing system that relies on the rapid production of click trains, or sequences of discrete clicks, to create an "acoustic image" of the environment from returning echoes. Odontocetes can emit high-intensity ultrasonic echolocation signals with maximum source levels exceeding 220 dB (Au 1993; Møhl et al. 2003), produce click trains consisting of up to several hundred clicks per second (Herzing 1996), and echolocate continuously (Branstetter et al. 2012). Numerous studies have demonstrated that sound overstimulation induces neural plasticity in the hippocampus and impairs hippocampal function (for review, Kraus and Canlon 2012). High-intensity sound exposure has been associated with alterations in hippocampal place cell activity (Goble et al. 2009), chronic suppression of hippocampal neurogenesis (Kraus et al. 2010), and even apoptosis of hippocampal neurons (Säljö et al. 2002). The mammalian hippocampus appears to be particularly vulnerable to auditory insult; thus, the routine exposure of odontocete cetaceans to high-intensity sounds during echolocation and communication may impact the development, structural integrity, and neurogenic capacity of their hippocampi selecting for an overall small size. The potentially significant influence of echolocation on hippocampal volume is further supported by findings that echolocating bats have smaller hippocampi than non-echolocating bats (Hutcheon et al. 2002). Furthermore, the Mysticeti also have diminutive hippocampi (Hof and Van Der Gucht 2007; Patzke et al. 2013) and produce high-intensity, low-frequency acoustic signals (Širović et al. 2007; Tyack 2000) associated with reproductive advertisement displays (Tyack and Clark 2000), as well as for long-range communication with conspecifics (Payne and Webb 1971; Clark and Ellison 2004), and potentially for orientation and navigation (Clark and Ellison 2004). Similar to mysticetes, *L. africana* produces high-intensity infrasonic signals for long-distance communication (Poole et al. 1988; Garstang 2010). Moreover, *L. africana* has the lowest relative hippocampal volume apart from cetaceans (Table 4). However, unlike cetaceans, *L. africana* exhibits hippocampal neurogenesis (Patzke et al. 2013). This suggests that both the production of high-intensity acoustic signals and the type of sound propagating medium (i.e., water or air) in which those signals are generated, each impact upon hippocampal morphology and function. Perhaps, the generation of high-intensity sound, whether ultra- or infrasonic, by cetaceans within a dense medium that accelerates and amplifies acoustic signals, is incompatible with sound-sensitive hippocampal tissue, potentially eliminating neurogenic capacity. This, in turn, may have necessitated an overall reduction of the cetacean hippocampus and indicates transfer of memory, learning, and navigational functions to neural structures less prone to acoustic injury, such as the entorhinal cortex or cerebellum.

Poor development of the odontocete hippocampus may also be associated with its potentially diminished function as a site of association and integration of multimodal (visual, auditory, olfactory, tactile, vestibular) sensory information (Mayes et al. 2007; Sweatt 2003). For odontocete cetaceans, olfactory input is absent, vestibular input is limited, and visual input is reduced. The most consistent and detailed spatial information available to odontocetes is acquired through audition. Odontocetes may not require spatial representations that integrate extensive information from multiple sensory stimuli to support navigation; instead, relying predominantly on acoustic information for spatial memory and orientation. Moreover, since odontocetes must attempt to localize mobile and patchily distributed prey species in a seemingly featureless aquatic environment, the utility of the hippocampus as a spatial mapping structure may be diminished. Ultimately, the role of the hippocampus as a multimodal association and integration site may no longer be of such utility in the odontocetes, potentially leading to the diminutive hippocampal size observed in this suborder.

Superior and inferior colliculi

In *O. orca*, the volume of the superior colliculi was 2.40 cm^3 comprising 0.04 % of the total brain volume (Table 1; Fig. 5). The inferior colliculi volume was 2.53 times larger than the volume of the superior colliculi, measuring 6.07 cm^3 and occupying 0.10 % of the total brain volume (Table 1; Fig. 5). A similar spatial relationship was observed for the maximal cross-sectional areas of the superior and inferior colliculi, with the maximal cross-sectional area of the inferior colliculi 2.25 times greater than that of the superior colliculi.

The superior and inferior colliculi are major sensory processing nodes within the midbrain. The inferior colliculus integrates acoustic information from various structures along the ascending and descending acoustic pathways (Casseday et al. 2002). Whereas, the superficial laminae of the superior colliculus are involved in visual processing (May 2006; Meredith and Stein 1986). The deep laminae of the superior colliculus integrate visual, auditory, and somatosensory inputs and mediate orientation responses toward sensory stimuli (Meredith and Stein 1986; Stein et al. 1989). The enlarged size of the inferior colliculi relative to the superior colliculi in *O. orca* is representative of the strong development of various components of the auditory system (for review, Oelschläger 2008) in the echolocating Odontoceti. In odontocete cetaceans, ratios of the maximal cross-sectional area of the inferior colliculi to superior colliculi range from 2:1 to 28:1 (Table 1). While in most non-echolocating Mysticeti, the superior colliculi are larger or approximately the same size as the inferior

colliculi (Oelschläger and Oelschläger 2009). Remarkably, in absolute terms, the inferior colliculi of *O. orca* are 6.46 times as large as those of *D. delphis*, the common dolphin, and nearly 80 times larger than the inferior colliculi of *H. sapiens* (Bullock and Gurevich 1979).

The dominant role of audition in the sensory repertoire of echolocating mammals is also apparent in the colliculi of microchiropteran bats which have hypertrophied inferior colliculi that exceed the superior colliculi in size (Covey and Casseday 1995; Hu et al. 2006). However, anatomical and neurophysiological studies of the microchiropteran superior colliculus suggest that this structure has evolved to function as a major auditory rather than visual sensori-motor interface, linking echoic spatial information to orienting behaviors (Covey et al. 1987; Valentine and Moss 1997; Sinha and Moss 2007). Though the extent of the superior colliculi of odontocete cetaceans is surpassed by that of the inferior colliculi, the potential evolution of acoustic specializations in the odontocete superior colliculi as observed in echolocating bats may ultimately confer to this structure greater relevance within the auditory system. While the odontocete superior colliculus may allocate considerable functional capacity to acoustic orientation by echolocation, behavioral evidence for cross-modal perception in *T. truncatus* (Pack and Herman 1995; Herman et al. 1998) suggests that the superior colliculus may also be an important site of multisensory integration in the Odontoceti.

A slight size asymmetry was observed between contralateral superior and inferior colliculi (Fig. 5). The volumes and maximal cross-sectional areas of the right superior (1.29 cm^3; 127.11 mm^2) and inferior (3.13 cm^3; 284.59 mm^2) colliculi were larger than the measurements for the left superior (1.11 cm^3; 108.42 mm^2) and inferior (2.94 cm^3; 246.27 mm^2) colliculi (Table 1). The asymmetry of the inferior colliculi in *O. orca* may be related to asymmetric cranial morphology, differential acoustic signaling mechanisms, and cerebral lateralization of function. Most odontocete crania exhibit varying degrees of asymmetry (Ness 1967; Dahlheim and Heyning 1999) potentially linked to the development of directional hearing in water (Fahlke et al. 2011). Furthermore, delphinids actively control acoustic signal dynamics through beam-steering (Moore et al. 2008) as well as preferentially utilize the right pair of phonic lips for generation of echolocation signals (clicks), and the left pair of phonic lips for production of communication signals (whistles; Madsen et al. 2013). The asymmetries of the inferior colliculi may reflect lateralized processing of behaviorally distinct acoustic stimuli as well as binaurally and spectrotemporally variant acoustic information arising from cranial asymmetry and active modification of cranial soft tissues. Evidence for neural circuit asymmetries in the perception of acoustic cues has

been collected for various mammalian species, including sea lions (Böye et al. 2005) and echolocating bats (Kanwal 2012; Washington and Kanwal 2012). Though studies of auditory lateralization have yet to be performed in odontocete cetaceans, there is an accumulating body of behavioral evidence for lateralized processing of social (Karenina et al. 2013a, b) and non-social (Yaman et al. 2003; von Fersen et al. 2000; Kilian et al. 2000) visual stimuli. Though the ubiquity and potential functional implications of collicular asymmetry in the Odontoceti awaits future investigation, it may be speculated that the size asymmetries observed in the superior and inferior colliculi of *O. orca* reflect lateralized processing of social and non-social acoustic information (e.g., communication whistles and echolocation clicks). Moreover, such functional asymmetry may bear some relevance to the detailed auditory localization ability demonstrated in *T. truncatus* by Renaud and Popper (1975).

Conclusions

There are some acknowledged limitations of the present study. Given the rarity of *O. orca* specimens, only one brain was available for morphometric analysis. While it is not suspected that the brain of this *O. orca* was anomalous for the species (i.e., this specimen is within the size range reported for adult male *O. orca*; Ridgway and Hanson 2014), due to the limited sample size of this study, future quantitative research examining *O. orca* specimens of varying sex, ontogenetic stage, and ecotype is required to increase the confidence of the present results and conclusions.

Volumetric measurements of neuroanatomy can be subject to error associated with postmortem processes, MRI, and segmentation. In the present study, volume deformation of the gray and white matter structures of this *O. orca* brain was likely mitigated by short postmortem interval (Montie et al. 2010) and imaging fresh, unfixed tissue within the neurocranium. However, limited local deformation was evident where cranial bone was cut to the dura mater. Additionally, CSF leakage from the neurocranium allowed for some positional shift of the brain. MRI acquisition artifacts, such as intensity inhomogeneity and partial-volume effect (i.e., multiple tissue types within a single voxel), may have contributed to error in gray and white matter tissue classification and substructure (e.g., subcortical nuclei and hippocampi) delineation. The very high resolution of this dataset limited partial-volume error due to the lower percentage of total voxels at the gray-white matter interface; however, volumetric overestimation and underestimation were still possible. Acquisition of ultra-high resolution 7 Tesla MRI data in future quantitative cetacean brain studies would mitigate such measurement errors and allow for neuroanatomical measurements of greater accuracy to be obtained. Lastly, manual segmentation of neuroanatomical structures is subjective. Segmentation error was reduced through consultation of various cetacean-specific and mammalian neuroanatomical atlases to determine structure boundaries and landmarks.

The present study, with its acknowledged caveats, has shown the potential for using MRI to examine cetacean neuroanatomy, and potential brain function and evolution. A unique neuroanatomical dataset for *O. orca*, heretofore absent from the literature, has resulted from this study. It is, therefore, particularly important for interspecific comparisons, and furnishes data which may be used to test hypotheses regarding cetacean brain structure, function, and evolution. This *O. orca* brain is one of the most corticalized (81.51 %, cerebrum volume occupying total brain volume) mammalian brains reported to date, and is representative of a species which may have the largest brain of all extant and extinct taxa (Ridgway and Hanson 2014). The divergent cerebral morphology of delphinoid cetaceans compared to other mammalian taxa may have evolved in response to the sensorimotor demands of the aquatic environment and may confer significant advantages for obligatory aquatic existence. Furthermore, environmental selective pressures associated with the evolution of echolocation and unihemispheric sleep have ostensibly altered substructure morphology and function. The delphinoid brain with its distinctive morphological features, cerebral scaling, and functional capacities offers fertile ground for future research concerning mammalian brain structure, function, and evolution. Moreover, the methodology of high resolution in situ MR imaging described in this study offers great promise for future investigation of cetacean brains.

References

Alonso-Farré J, Gonzalo-Orden M, Barreiro-Vázquez J, Barreiro-Lois A, André M, Morell M, Llarena-Reino M, Monreal-Pawlowsky T, Degollada E (2014) Cross-sectional anatomy, computed tomography and magnetic resonance imaging of the head of common dolphin (*Delphinus delphis*) and Striped Dolphin (*Stenella coeruleoalba*). Anat Histol Embryol 44(1):13–21

Anthony R (1938) Essai de recherche d'une expression anatomique approximative du degré d'organisation cérébrale, autre que le poids de l'encéphale comparé au poids du corps. B Mem Soc Anthro Par 9(1):17–67

Au W (1993) Characteristics of dolphin sonar signals. The sonar of dolphins. Springer, New York, pp 115–139

Au W, Nachtigall P (1997) Acoustics of echolocating dolphins and small whales. Mar Freshw Behav Phys 29(1–4):127–162

Barton R (1998) Visual specialization and brain evolution in primates. Philos Roy Soc B 265(1409):1933–1937

Barton R (2006) Primate brain evolution: integrating comparative, neurophysiological, and ethological data. Evol Anthropol 15(6):224–236

Barton R, Capellini I (2011) Maternal investment, life histories, and the costs of brain growth in mammals. P Natl Acad Sci 108(15):6169–6174

Barton R, Harvey P (2000) Mosaic evolution of brain structure in mammals. Nature 405(6790):1055–1058

Bassett D, Bullmore E (2006) Small-world brain networks. Neuroscientist 12(6):512–523

Begeman L, St. Leger J, Blyde D, Jauniaux T, Lair S, Lovewell G, Raverty S, Seibel H, Siebert U, Staggs S (2012) Intestinal volvulus in cetaceans. Vet Pathol 50(4):590–596

Berns G, Cook P, Foxley S, Jbabdi S, Miller K, Marino L (2015) Diffusion tensor imaging of dolphin brains reveals direct auditory pathway to temporal lobe. Proc R Soc B 282:20151203

Block B, Jonsen I, Jorgensen S, Winship A, Shaffer S, Bograd S, Hazen E, Foley D, Breed G, Harrison A (2011) Tracking apex marine predator movements in a dynamic ocean. Nature 475(7354):86–90

Bohonak A, van der Linde K (2004) RMA: software for reduced major axis regression. http://www.bio.sdsu.edu/pub/andy/rma.html. Accessed 10 Feb 2015

Böye M, Güntürkün O, Vauclair J (2005) Right ear advantage for conspecific calls in adults and subadults, but not infants, California sea lions (*Zalophus californianus*): hemispheric specialization for communication? Eur J Neurosci 21(6):1727–1732

Branstetter B, Finneran J, Fletcher E, Weisman B, Ridgway S (2012) Dolphins can maintain vigilant behavior through echolocation for 15 days without interruption or cognitive impairment. PLoS One 7(10):e47478

Bullock T, Gurevich V (1979) Soviet literature on the nervous system and psychobiology of Cetacea. Int Rev Neurobiol 21:47–127

Burgess N, Maguire E, O'Keefe J (2002) The human hippocampus and spatial and episodic memory. Neuron 35(4):625–641

Butti C, Janeway C, Townshend C, Wicinski B, Reidenberg J, Ridgway S, Sherwood C, Hof P, Jacobs B (2014a) The neocortex of cetartiodactyls: I. A comparative Golgi analysis of neuronal morphology in the bottlenose dolphin (*Tursiops truncatus*), the minke whale (*Balaenoptera acutorostrata*), and the humpback whale (*Megaptera novaeangliae*). Brain Struct Funct 220(6):3339–3368

Butti C, Raghanti M, Gu X, Bonar C, Wicinski B, Wong E, Roman J, Brake A, Eaves E, Spocter M (2014b) The cerebral cortex of the pygmy hippopotamus, *Hexaprotodon liberiensis* (Cetartiodactyla, Hippopotamidae): MRI, cytoarchitecture, and neuronal morphology. Anat Rec 297(4):670–700

Byrne R, Bates L (2007) Sociality, evolution and cognition. Curr Biol 17(16):R714–R723

Casseday J, Fremouw T, Covey E (2002) The inferior colliculus: a hub for the central auditory system. Integrative functions in the mammalian auditory pathway. Springer, Berlin, pp 238–318

Changizi M (2001) Principles underlying mammalian neocortical scaling. Biol Cybern 84(3):207–215

Charvet C, Finlay B (2012) Embracing covariation in brain evolution: large brains, extended development, and flexible primate social systems. Prog Brain Res 195:71–87

Charvet C, Striedter G, Finlay B (2011) Evo-devo and brain scaling: candidate developmental mechanisms for variation and constancy in vertebrate brain evolution. Brain Behav Evol 78(3):248–257

Chen Y (1979) On the cerebral anatomy of the Chinese river dolphin, *Lipotes vexillifer* Miller. Acta Hydrob Sin 4:365–372

Clark C, Ellison W (2004) Potential use of low-frequency sounds by baleen whales for probing the environment: evidence from models and empirical measurements. In: Thomas J, Moss C, Vater M (eds) Echolocation in bats and dolphins. The University of Chicago Press, Chicago, pp 564–582

Clark D, Mitra P, Wang S (2001) Scalable architecture in mammalian brains. Nature 411(6834):189–193

Connor R (2007) Dolphin social intelligence: complex alliance relationships in bottlenose dolphins and a consideration of selective environments for extreme brain size evolution in mammals. Philos Trans R Soc B 362:587–602

Cooper F, Grube M, Von Kriegstein K, Kumar S, English P, Kelly T, Chinnery P, Griffiths T (2012) Distinct critical cerebellar subregions for components of verbal working memory. Neuropsychologia 50(1):189–197

Covey E, Casseday J (1995) The lower brainstem auditory pathways. Hearing by bats. Springer, New York, pp 235–295

Covey E, Hall W, Kobler J (1987) Subcortical connections of the superior colliculus in the mustache bat, *Pteronotus parnellii*. J Comp Neurol 263(2):179–197

Dahlheim M, Heyning J (1999) Killer Whale— *Orcinus orca* (Linnaeus, 1758). In: Ridgway S, Harrison R (eds) Handbook of marine mammals: the second book of dolphins and porpoises, vol 6. Academic Press, London

Dawson W, Hawthorne M, Jenkins R, Goldston R (1982) Giant neural systems in the inner retina and optic nerve of small whales. J Comp Neurol 205(1):1–7

De Graaf A (1967) Anatomical aspects of the cetacean brain stem, vol 5. Royal VanGorcum Ltd., The Netherlands

Dunbar R (1998) The social brain hypothesis. Brain 9:178–190

Durban J, Pitman R (2012) Antarctic killer whales make rapid, round-trip movements to subtropical waters: evidence for physiological maintenance migrations? Biol Lett 8(2):274–277

Eriksen N, Pakkenberg B (2007) Total neocortical cell number in the mysticete brain. Anat Rec 290(1):83–95

Fahlke J, Gingerich P, Welsh R, Wood A (2011) Cranial asymmetry in *Eocene archaeocete* whales and the evolution of directional hearing in water. Proc Natl Acad Sci 108(35):14545–14548

Fears S, Melega W, Lee C, Chen K, Tu Z, Jorgensen M, Fairbanks L, Cantor R, Freimer N, Woods R (2009) Identifying heritable brain phenotypes in an extended pedigree of vervet monkeys. J Neurosci 29(9):2867–2875

Gao G, Zhou K (1991) The number of fibers and range of fiber diameters in the cochlear nerve of three odontocete species. Can J Zool 69(9):2360–2364

Gao G, Zhou K (1992) Fiber analysis of the optic and cochlear nerves of small cetaceans. Marine mammal sensory systems. Springer, Berlin, pp 39–52

Garstang M (2010) Elephant infrasounds: long-range communication. In: Brudzynski S (ed) Handbook of mammalian vocalization—

an integrative neuroscience approach, vol 19. Elsevier, Oxford, pp 57–67

Gatesy J, Geisler J, Chang J, Buell C, Berta A, Meredith R, Springer M, McGowen M (2013) A phylogenetic blueprint for a modern whale. Mol Phylogenet Evol 66(2):479–506

Gihr M, Pilleri G (1969) On the anatomy and biometry of *Stenella styx* Gray and *Delphinus delphis* L. (*Cetacea*, Delphinidae) of the western Mediterranean. Investig Cetacea 1:15–65

Gilissen E (2006) Scaling patterns of interhemispheric connectivity in eutherian mammals. Behav Brain Sci 29:16–17

Goble T, Møller A, Thompson L (2009) Acute high-intensity sound exposure alters responses of place cells in hippocampus. Hear Res 253(1):52–59

Goley P (1999) Behavioral aspects of sleep in Pacific White-Sided Dolphins (*Lagenorhynchus obliquidens*, Gill 1865). Mar Mamm Sci 15(4):1054–1064

Gompertz R (1902) Specific gravity of the brain. J Physiol 27(6):459–462

Gruenberger H (1970) On the cerebral anatomy of the Amazon dolphin, *Inia geoffrensis*. Investig Cetacea 2:129–144

Habas C, Kamdar N, Nguyen D, Prater K, Beckmann C, Menon V, Greicius M (2009) Distinct cerebellar contributions to intrinsic connectivity networks. J Neurosci 29(26):8586–8594

Haddad D, Huggenberger S, Haas-Rioth M, Kossatz L, Oelschläger H, Haase A (2012) Magnetic resonance microscopy of prenatal dolphins (Mammalia, Odontoceti, Delphinidae)—ontogenetic and phylogenetic implications. Zool Anz 251(2):115–130

Hakeem A, Hof P, Sherwood C, Switzer R, Rasmussen L, Allman J (2005) Brain of the African elephant (*Loxodonta africana*): neuroanatomy from magnetic resonance images. Anat Rec A 287(1):1117–1127

Hanson A, Grisham W, Sheh C, Annese J, Ridgway S (2013) Quantitative examination of the bottlenose dolphin cerebellum. Anat Rec 296:1215–1228

Haug H (1970) Der makroskopische Aufbau des Großhirns: qualitative und quantitative Untersuchungen an den Gehirnen des Menschen, der Delphinoideae und des Elefanten. ERG ANAT ENTW, vol 43(4). Springer, Berlin. Accessed 17 Feb 2015

Herculano-Houzel S (2011) Brains matter, bodies maybe not: the case for examining neuron numbers irrespective of body size. Ann NY Acad Sci 1225(1):191–199

Herculano-Houzel S (2014) The glia/neuron ratio: how it varies uniformly across brain structures and species and what that means for brain physiology and evolution. Glia 62(9):1377–1391

Herculano-Houzel S, Avelino-de-Souza K, Neves K, Porfírio J, Messeder D, Feijó L, Maldonado J, Manger P (2014) The elephant brain in numbers. Front Neuroanat 8:46. Accessed 30 Sep 2015

Herman L (2010) What laboratory research has told us about dolphin cognition. Int J Comp Psychol 23(3):310–330

Herman L, Pack A, Hoffmann-Kuhnt M (1998) Seeing through sound: Dolphins (*Tursiops truncatus*) perceive the spatial structure of objects through echolocation. J Comp Psychol 112(3):292–305

Herzing D (1996) Vocalizations and associated underwater behavior of free-ranging Atlantic spotted dolphins, *Stenella frontalis* and bottlenose dolphins, *Tursiops truncatus*. Aquat Mamm 22:61–80

Hof P, Van Der Gucht E (2007) Structure of the cerebral cortex of the humpback whale, *Megaptera novaeangliae* (Cetacea, Mysticeti, Balaenopteridae). Anat Rec 290(1):1–31

Hof P, Chanis R, Marino L (2005) Cortical complexity in cetacean brains. Anat Rec A 287(1):1142–1152

Hofman M (1985) Size and shape of the cerebral cortex in mammals: I. The cortical surface. Brain Behav Evol 27(1):28–40

Hofman M (1988) Size and shape of the cerebral cortex in mammals. Brain Behav Evol 32(1):17–26

Hofman M (1989) On the evolution and geometry of the brain in mammals. Prog Neurobiol 32(2):137–158

Hofman M (2012) Design principles of the human brain: an evolutionary perspective. Prog Brain Res 195:373–390

Hofman M, Laan A, Uylings H (1986) Bivariate linear models in neurobiology: problems of concept and methodology. J Neurosci Methods 18(1):103–114

Hu K, Li Y, Gu X, Lei H, Zhang S (2006) Brain structures of echolocating and nonecholocating bats, derived in vivo from magnetic resonance images. Neuroreport 17(16):1743–1746

Hursh J (1939) Conduction velocity and diameter of nerve fibers. Am J Physiol 127:131–139

Hutcheon J, Kirsch J, Garland T (2002) A comparative analysis of brain size in relation to foraging ecology and phylogeny in the chiroptera. Brain Behav Evol 60(3):165–180

Jacobs M, Jensen A (1964) Gross aspects of the brain and a fiber analysis of cranial nerves in the great whale. J Comp Neurol 123(1):55–71

Jacobs M, McFarland W, Morgane P (1979) The anatomy of the brain of the bottlenose dolphin (*Tursiops truncatus*). Rhinic lobe (rhinencephalon): the archicortex. Brain Res Bull 4(1):1–108

Joffe T (1997) Social pressures have selected for an extended juvenile period in primates. J Hum Evol 32(6):593–605

Kanwal J (2012) Right–left asymmetry in the cortical processing of sounds for social communication vs. navigation in mustached bats. Eur J Neurosci 35(2):257–270

Karenina K, Giljov A, Glazov D, Malashichev Y (2013a) Social laterality in wild beluga whale infants: comparisons between locations, escort conditions, and ages. Behav Ecol Sociobiol 67(7):1195–1204

Karenina K, Giljov A, Ivkovich T, Burdin A, Malashichev Y (2013b) Lateralization of spatial relationships between wild mother and infant orcas, *Orcinus orca*. Anim Behav 86(6):1225–1231

Kazu R, Maldonado J, Mota B, Manger P, Herculano-Houzel S (2014) Cellular scaling rules for the brain of Artiodactyla include a highly folded cortex with few neurons. Front Neuroanat 8:128. Accessed 7 Oct 2015

Keogh M, Ridgway S (2008) Neuronal fiber composition of the corpus callosum within some odontocetes. Anat Rec 291(7):781–789

Kilian A, von Fersen L, Güntürkün O (2000) Lateralization of visuospatial processing in the bottlenose dolphin (*Tursiops truncatus*). Behav Brain Res 116(2):211–215

Knoops A, Gerritsen L, van der Graaf Y, Mali W, Geerlings M (2010) Basal hypothalamic pituitary adrenal axis activity and hippocampal volumes: the SMART-Medea study. Biol Psychiatr 67(12):1191–1198

Kraus K, Canlon B (2012) Neuronal connectivity and interactions between the auditory and limbic systems. Effects of noise and tinnitus. Hear Res 288(1):34–46

Kraus K, Mitra S, Jimenez Z, Hinduja S, Ding D, Jiang H, Gray L, Lobarinas E, Sun W, Salvi R (2010) Noise trauma impairs neurogenesis in the rat hippocampus. Neurosci 167(4):1216–1226

Kretschmann H, Tafesse U, Herrmann A (1982) Different volume changes of cerebral cortex and white matter during histological preparation. Microsc Acta 86(1):13–24

Ladygina T, Mass A, Supin A (1978) Multiple sensory projections in the dolphin cerebral cortex. Zh Vyssh Nerv Deyat 28(5):1047–1053

Larsell O (1970) The comparative anatomy and histology of the cerebellum: from monotremes through apes, vol 2. University Of Minnesota Press, Minneapolis

Lyamin O, Manger P, Ridgway S, Mukhametov L, Siegel J (2008) Cetacean sleep: an unusual form of mammalian sleep. Neurosci Biobehav Rev 32(8):1451–1484

MacNeilage P (2013) Vertebrate whole-body-action asymmetries and the evolution of right handedness: a comparison between humans and marine mammals. Dev Psychobiol 55(6):577–587

Madsen P, Lammers M, Wisniewska D, Beedholm K (2013) Nasal sound production in echolocating delphinids (*Tursiops truncatus* and *Pseudorca crassidens*) is dynamic, but unilateral: clicking on the right side and whistling on the left side. J Exp Biol 216(21):4091–4102

Manger P (2006) An examination of cetacean brain structure with a novel hypothesis correlating thermogenesis to the evolution of a big brain. Biol Rev 81(02):293–338

Manger P (2013) Questioning the interpretations of behavioral observations of cetaceans: is there really support for a special intellectual status for this mammalian order? Neurosci 250:664–696

Manger P, Hemingway J, Haagensen M, Gilissen E (2010) Cross-sectional area of the elephant corpus callosum: comparison to other eutherian mammals. Neuroscience 167(3):815–824

Manger P, Prowse M, Haagensen M, Hemingway J (2012) Quantitative analysis of neocortical gyrencephaly in African elephants (*Loxodonta africana*) and six species of cetaceans: comparison with other mammals. J Comp Neurol 520(11):2430–2439

Marino L (1998) A comparison of encephalization between odontocete cetaceans and anthropoid primates. Brain Behav Evol 51(4):230–238

Marino L, Rilling J, Lin S, Ridgway S (2000) Relative volume of the cerebellum in dolphins and comparison with anthropoid primates. Brain Behav Evol 56(4):204–211

Marino L, Murphy T, Deweerd A, Morris J, Fobbs A, Humblot N, Ridgway S, Johnson J (2001a) Anatomy and three-dimensional reconstructions of the brain of the white whale (*Delphinapterus leucas*) from magnetic resonance images. Anat Rec 262(4):429–439

Marino L, Murphy T, Gozal L, Johnson J (2001b) Magnetic resonance imaging and three-dimensional reconstructions of the brain of a fetal common dolphin, *Delphinus delphis*. Anat Embryol 203(5):393–402

Marino L, Sudheimer K, Murphy T, Davis K, Pabst D, McLellan W, Rilling J, Johnson J (2001c) Anatomy and three-dimensional reconstructions of the brain of a bottlenose dolphin (*Tursiops truncatus*) from magnetic resonance images. Anat Rec 264(4):397–414

Marino L, Sudheimer K, Pabst D, Mclellan W, Filsoof D, Johnson J (2002) Neuroanatomy of the common dolphin (*Delphinus delphis*) as revealed by magnetic resonance imaging (MRI). Anat Rec 268(4):411–429

Marino L, Sudheimer K, Sarko D, Sirpenski G, Johnson J (2003) Neuroanatomy of the harbor porpoise (*Phocoena phocoena*) from magnetic resonance images. J Morphol 257(3):308–347

Marino L, McShea D, Uhen M (2004a) Origin and evolution of large brains in toothed whales. Anat Rec A 281(2):1247–1255

Marino L, Sherwood C, Delman B, Tang C, Naidich T, Hof P (2004b) Neuroanatomy of the killer whale (*Orcinus orca*) from magnetic resonance images. Anat Rec A 281(2):1256–1263

Marino L, Sudheimer K, Mclellan W, Johnson J (2004c) Neuroanatomical structure of the spinner dolphin (*Stenella longirostris orientalis*) brain from magnetic resonance images. Anat Rec A 279(1):601–610

Marino L, Sudheimer K, Pabst D, McLellan W, Arshad S, Naini G, Johnson J (2004d) Anatomical description of an infant bottlenose dolphin (*Tursiops truncatus*) brain from magnetic resonance images. Aquat Mamm 30(2):315–326

Marino L, Butti C, Connor R, Fordyce R, Herman L, Hof P, Lefebvre L, Lusseau D, McCowan B, Nimchinsky E (2008) A claim in search of evidence: reply to Manger's thermogenesis hypothesis of cetacean brain structure. Biol Rev 83(4):417–440

Marrif H, Juurlink B (1999) Astrocytes respond to hypoxia by increasing glycolytic capacity. J Neurosci Res 57(2):255–260

Martín E, Fernández M, Perea G, Pascual O, Haydon P, Araque A, Ceña V (2007) Adenosine released by astrocytes contributes to hypoxia-induced modulation of synaptic transmission. Glia 55(1):36–45

Maximino C (2009a) A quantitative test of the thermogenesis hypothesis of cetacean brain evolution, using phylogenetic comparative methods. Mar Freshw Behav Phy 42(1):1–17

Maximino C (2009b) Reply to Manger's Commentary on "A quantitative test of the thermogenesis hypothesis of cetacean brain evolution, using phylogenetic comparative methods". Mar Freshw Behav Phy 42(5):363–372

May P (2006) The mammalian superior colliculus: laminar structure and connections. Prog Brain Res 151:321–378

Mayes A, Montaldi D, Migo E (2007) Associative memory and the medial temporal lobes. Trends Cogn Sci 11(3):126–135

Mazzatenta A, Caleo M, Baldaccini N, Maffei L (2001) A comparative morphometric analysis of the optic nerve in two cetacean species, the striped dolphin (*Stenella coeruleoalba*) and fin whale (*Balaenoptera physalus*). Vis Neurosci 18:319–325

McArdle B (1988) The structural relationship: regression in biology. Can J Zool 66(11):2329–2339

McFarland W, Morgane P, Jacobs M (1969) Ventricular system of the brain of the dolphin, *Tursiops truncatus*, with comparative anatomical observations and relations to brain specializations. J Comp Neurol 135(3):275–367

McHugh T, Saykin A, Wishart H, Flashman L, Cleavinger H, Rabin L, Mamourian A, Shen L (2007) Hippocampal volume and shape analysis in an older adult population. Clin Neuropsychol 21(1):130–145

Meredith M, Stein B (1986) Visual, auditory, and somatosensory convergence on cells in superior colliculus results in multisensory integration. J Neurophysiol 56(3):640–662

Meyer J (1981) A quantitative comparison of the parts of the brains of two Australian marsupials and some eutherian mammals. Brain Behav Evol 18(1–2):60–71

Møhl B, Wahlberg M, Madsen P, Heerfordt A, Lund A (2003) The monopulsed nature of sperm whale clicks. J Acoust Soc Am 114(2):1143–1154

Montie E, Schneider G, Ketten D, Marino L, Touhey K, Hahn M (2007) Neuroanatomy of the subadult and fetal brain of the Atlantic White-sided Dolphin (*Lagenorhynchus acutus*) from in situ magnetic resonance images. Anat Rec 290(12):1459–1479

Montie E, Schneider G, Ketten D, Marino L, Touhey K, Hahn M (2008) Volumetric neuroimaging of the Atlantic White-Sided Dolphin (*Lagenorhynchus acutus*) brain from in situ magnetic resonance images. Anat Rec 291(3):263–282

Montie E, Wheeler E, Pussini N, Battey T, Barakos J, Dennison S, Colegrove K, Gulland F (2010) Magnetic resonance imaging quality and volumes of brain structures from live and post-mortem imaging of California sea lions with clinical signs of domoic acid toxicosis. Dis Aquat Org 91(3):243–256

Moore P, Dankiewicz L, Houser D (2008) Beamwidth control and angular target detection in an echolocating bottlenose dolphin (*Tursiops truncatus*). J Acoust Soc Am 124(5):3324–3332

Morey R, Petty C, Xu Y, Hayes J, Wagner H II, Lewis D, LaBar K, Styner M, McCarthy G (2009) A comparison of automated segmentation and manual tracing for quantifying hippocampal and amygdala volumes. Neuroimage 45(3):855–866

Morgane P, McFarland W, Jacobs M (1982) The limbic lobe of the dolphin brain: a quantitative cytoarchitectonic study. J Hirnforsch 23(5):465–552

Mortensen H, Pakkenberg B, Dam M, Dietz R, Sonne C, Mikkelsen B, Eriksen N (2014) Quantitative relationships in delphinid neocortex. Front Neuroanat 8:1–10

Ness A (1967) A measure of asymmetry of the skulls of odontocete whales. J Zool 153(2):209–221

Nummela S, Wägar T, Hemilä S, Reuter T (1999) Scaling of the cetacean middle ear. Hear Res 133(1):71–81

Oelschläger H (2008) The dolphin brain—a challenge for synthetic neurobiology. Brain Res Bull 75(2):450–459

Oelschläger H, Oelschläger J (2009) Brain. In: Perrin WF, Wursig B, Thewissen J (eds) Encyclopedia of marine mammals. Elsevier, Oxford

Oelschläger H, Haas-Rioth M, Fung C, Ridgway S, Knauth M (2007) Morphology and evolutionary biology of the dolphin (Delphinus sp.) brain—MR imaging and conventional histology. Brain Behav Evol 71(1):68–86

Oelschläger H, Ridgway S, Knauth M (2010) Cetacean brain evolution: Dwarf sperm whale (Kogia sima) and common dolphin (Delphinus delphis)–an investigation with high-resolution 3D MRI. Brain Behav Evol 75:33–62

Pack A, Herman L (1995) Sensory integration in the bottle nosed dolphin: immediate recognition of complex shapes across the senses of echolocation and vision. J Acoust Soc Am 98(2): 722–733

Pakkenberg B, Gundersen H (1997) Neocortical neuron number in humans: effect of sex and age. J Comp Neurol 384:312–320

Panin M, Gabai G, Ballarin C, Peruffo A, Cozzi B (2012) Evidence of melatonin secretion in cetaceans: plasma concentration and extrapineal HIOMT-like presence in the bottlenose dolphin Tursiops truncatus. Gen Comp Endocr 177(2):238–245

Patzke N, Spocter M, Bertelsen M, Haagensen M, Chawana R, Streicher S, Kaswera C, Gilissen E, Alagaili A, Mohammed O (2013) In contrast to many other mammals, cetaceans have relatively small hippocampi that appear to lack adult neurogenesis. Brain Struct Funct 1–23. Accessed 7 Oct 2015

Payne R, Webb D (1971) Orientation by means of long range acoustic signaling in baleen whales. Ann NY Acad Sci 188(1):110–141

Pfrieger F, Barres B (1997) Synaptic efficacy enhanced by glial cells in vitro. Science 277(5332):1684–1687

Pierson R, Corson P, Sears L, Alicata D, Magnotta V, O'Leary D, Andreasen N (2002) Manual and semiautomated measurement of cerebellar subregions on MR images. Neuroimage 17(1):61–76

Pilleri G (1972) Cerebral anatomy of the Platanistidae (Platanista gangetica, Platanista indi, Pontoporia blainvillei, Inia geoffrensis). Investig Cetacea 4:44–70

Pilleri G, Gihr M (1969) On the anatomy and behaviour of Risso's dolphin (Grampus griseus G. Cuvier). Investig Cetacea 1:74-93. Accessed 26 Jan 2015

Pilleri G, Gihr M (1970) The central nervous system of the mysticete and odontocete whales. Investig Cetacea 2:87–135

Pilleri G, Gihr M (1972) Contribution to the knowledge of the cetaceans of Pakistan with particular reference to the genera Neomeris, Sousa, Delphinus, and Tursiops and description of a new Chinese porpoise (Neomeris asiaeorientalis). Investig Cetacea 4:107–162

Pirlot P, Kamiya T (1985) Qualitative and quantitative brain morphology in the Sirenian Dugong dugong Erxl. J Zool Syst Evol Res 23(2):147–155

Poole J, Payne K, Langbauer W, Moss C (1988) The social contexts of some very low frequency calls of African elephants. Behav Ecol Sociobiol 22(6):385–392

Poth C, Fung C, Güntürkün O, Ridgway S, Oelschläger H (2005) Neuron numbers in sensory cortices of five delphinids compared to a physeterid, the pygmy sperm whale. Brain Res Bull 66(4):357–360

Quester R, Schröder R (1997) The shrinkage of the human brain stem during formalin fixation and embedding in paraffin. J Neurosci Meth 75(1):81–89

Rattenborg N, Amlaner C, Lima S (2000) Behavioral, neurophysiological and evolutionary perspectives on unihemispheric sleep. Neurosci Biobehav Rev 24(8):817–842

Reader S, Laland K (2002) Social intelligence, innovation, and enhanced brain size in primates. Proc Nat Acad Sci 99(7): 4436–4441

Reep R, O'Shea T (1990) Regional brain morphometry and lissencephaly in the Sirenia. Brain Behav Evol 35(4):185–194

Reep R, Finlay B, Darlington R (2007) The limbic system in mammalian brain evolution. Brain Behav Evol 70:57–70

Renaud D, Popper A (1975) Sound localization by the bottlenose porpoise Tursiops truncatus. J Exp Biol 63(3):569–585

Ridgway S (1986) Physiological observations on dolphin brains. In: Schusterman R, Thomas J, Wood F (eds) Dolphin cognition and behavior: a comparative approach. pp 31–60. Accessed 26 Jan 2015

Ridgway S (1990) The central nervous system of the bottlenose dolphin. In: Leatherwood S, Reeves R (eds) The bottlenose dolphin. pp 69–97. Accessed 8 Nov 2013

Ridgway S (2000) The auditory central nervous system of dolphins. In: Au W, Popper A, Fay R (eds) Hearing by whales and dolphins. Springer, New York, pp 273–293

Ridgway S, Brownson R (1984) Relative brain sizes and cortical surface areas in odontocetes. Acta Zool Fenn 172:149–152

Ridgway S, Hanson A (2014) Sperm whales and killer whales with the largest brains of all toothed whales show extreme differences in cerebellum. Brain Behav Evol 83(4):1–9

Ridgway S, Tarpley R (1996) Brain mass comparisons in Cetacea. Proc Int Assoc Aquat Anim Med 27:55–57

Ridgway S, Bullock T, Carder D, Seeley R, Woods D, Galambos R (1981) Auditory brainstem response in dolphins. Proc Natl Acad Sci 78(3):1943–1947

Ridgway S, Marino L, Lipscomb T (2002) Description of a poorly differentiated carcinoma within the brainstem of a white whale (Delphinapterus leucas) from magnetic resonance images and histological analysis. Anat Rec 268(4):441–449

Ridgway S, Houser D, Finneran J, Carder D, Keogh M, Van Bonn W, Smith C, Scadeng M, Dubowitz D, Mattrey R (2006) Functional imaging of dolphin brain metabolism and blood flow. J Exp Biol 209(15):2902–2910

Rilling J, Insel T (1999a) Differential expansion of neural projection systems in primate brain evolution. Neuroreport 10(7): 1453–1459

Rilling J, Insel T (1999b) The primate neocortex in comparative perspective using magnetic resonance imaging. J Hum Evol 37(2):191–223

Ringo J (1991) Neuronal interconnection as a function of brain size. Brain Behav Evol 38(1):1–6

Roth G, Dicke U (2005) Evolution of the brain and intelligence. Trends Cogn Sci 9(5):250–257

Ruscher K, Freyer D, Karsch M, Isaev N, Megow D, Sawitzki B, Priller J, Dirnagl U, Meisel A (2002) Erythropoietin is a paracrine mediator of ischemic tolerance in the brain: evidence from an in vitro model. J Neurosci 22(23):10291–10301

Säljö A, Bao F, Jingshan S, Hamberger A, Hansson H, Haglid K (2002) Exposure to short-lasting impulse noise causes neuronal c-Jun expression and induction of apoptosis in the adult rat brain. J Neurotraum 19(8):985–991

Schlenska G (1974) Volumen und Oberflächenmessungen an Gehirnen verschiedener Säugetiere im Vergleich zu einem errechneten Modell. J Hirnforsch 15:401–408

Schulz G, Crooijmans H, Germann M, Scheffler K, Müller-Gerbl M, Müller B (2011) Three-dimensional strain fields in human brain resulting from formalin fixation. J Neurosci Methods 202(1): 17–27

Seiffert E (2007) A new estimate of afrotherian phylogeny based on simultaneous analysis of genomic, morphological, and fossil evidence. BMC Evol Biol 7(1):224

Shoshani J, Kupsky W, Marchant G (2006) Elephant brain: Part I: gross morphology, functions, comparative anatomy, and evolution. Brain Res Bull 70(2):124–157

Shultz S, Dunbar R (2006) Both social and ecological factors predict ungulate brain size. Proc R Soc B 273(1583):207–215

Sinha S, Moss C (2007) Vocal premotor activity in the superior colliculus. J Neurosci 27(1):98–110

Širović A, Hildebrand J, Wiggins S (2007) Blue and fin whale call source levels and propagation range in the Southern Ocean. J Acoust Soc Am 122(2):1208–1215

Smith R (2005) Relative size versus controlling for size. Curr Anthropol 46(2):249–273

Stein B, Meredith M, Huneycutt W, McDade L (1989) Behavioral indices of multisensory integration: orientation to visual cues is affected by auditory stimuli. J Cogn Neurosci 1(1):12–24

Stephan H (1960) Methodische studien über den quantitativen vergleich architektonischer struktureinheiten des gehirns. Z Wiss Zool 164:143–172

Stephan H, Frahm H, Baron G (1981) New and revised data on volumes of brain structures in insectivores and primates. Folia Primatol 35:1–29

Swanson R, Farrell K, Stein B (1997) Astrocyte energetics, function, and death under conditions of incomplete ischemia: a mechanism of glial death in the penumbra. Glia 21(1):142–153

Sweatt J (2003) The hippocampus serves a role in multimodal information processing, and memory consolidation. Mechanisms of memory. Elsevier Academic Press, Oxford

Tarpley R, Ridgway S (1994) Corpus callosum size in delphinid cetaceans. Brain Behav Evol 44(3):156–165

Tyack P (1999) Communication and cognition. In: Reynolds JE, Rommel SA (eds) Biology of marine mammals. Smithsonian Institution Press, Washington, pp 287–323

Tyack P (2000) Functional aspects of cetacean communication. In: Mann J, Connor R, Tyack P, Whitehead H (eds) Cetacean societies: field studies of dolphins and whales. University of Chicago Press, Chicago, pp 270–307

Tyack P, Clark C (2000) Communication and acoustic behavior of dolphins and whales. In: Au W, Popper A, Fay R (eds) Hearing by whales and dolphins. Springer, New York, pp 156–224

Ullian E, Sapperstein S, Christopherson K, Barres B (2001) Control of synapse number by glia. Science 291(5504):657–661

Valentine D, Moss C (1997) Spatially selective auditory responses in the superior colliculus of the echolocating bat. J Neurosci 17(5):1720–1733

Verkhratsky A, Butt A (2013) Neuroglia: definition, classification, evolution, numbers, development. Glial physiology and pathophysiology, 1st edn. Wiley, New York, pp 73–104

von Fersen L, Schall U, Güntürkün O (2000) Visual lateralization of pattern discrimination in the bottlenose dolphin (Tursiops truncatus). Behav Brain Res 107(1):177–181

Walhovd K, Westlye L, Amlien I, Espeseth T, Reinvang I, Raz N, Agartz I, Salat D, Greve D, Fischl B (2011) Consistent neuroanatomical age-related volume differences across multiple samples. Neurobiol Aging 32(5):916–932

Walløe S, Eriksen N, Dabelsteen T, Pakkenberg B (2010) A neurological comparative study of the harp seal (Pagophilus groenlandicus) and harbor porpoise (Phocoena phocoena) brain. Anat Rec 293(12):2129–2135

Wartzok D, Ketten D (1999) Marine mammal sensory systems. In: Reynolds J, Rommel S (eds) Biology of marine mammals. Smithsonian Institution Press, Washington, pp 117–174

Washington S, Kanwal J (2012) Sex-dependent hemispheric asymmetries for processing frequency-modulated sounds in the primary auditory cortex of the mustached bat. J Neurophysiol 108(6):1548–1566

Watts D, Strogatz S (1998) Collective dynamics of 'small-world' networks. Nature 393(6684):440–442

Waxman S (1980) Determinants of conduction velocity in myelinated nerve fibers. Muscle Nerve 3(2):141–150

Wen Q, Chklovskii D (2005) Segregation of the brain into gray and white matter: a design minimizing conduction delays. Plos Comput Biol 1(7):e78

Whitehead H, Mann J (2000) Female reproductive strategies of cetaceans. In: Mann J, Connor R, Tyack P, Whitehead H (eds) Cetacean societies: field studies of dolphins and whales. University of Chicago Press, Chicago, pp 219–246

Wislocki G (1929) The hypophysis of the porpoise (Tursiops truncatus). Arch Surg 18(4):1403–1412

Würsig B (2009) Intelligence and cognition. In: Perrin W, Würsig B, Thewissen J (eds) Encyclopedia of marine mammals, 2nd edn. Academic Press, Cambridge, pp 616–623

Yaman S, von Fersen L, Dehnhardt G, Güntürkün O (2003) Visual lateralization in the bottlenose dolphin (Tursiops truncatus): evidence for a population asymmetry? Behav Brain Res 142(1):109–114

Yamazaki Y, Hozumi Y, Kaneko K, Sugihara T, Fujii S, Goto K, Kato H (2007) Modulatory effects of oligodendrocytes on the conduction velocity of action potentials along axons in the alveus of the rat hippocampal CA1 region. Neuron Glia Biol 3(04):325–334

Zhang K, Sejnowski T (2000) A universal scaling law between gray matter and white matter of cerebral cortex. Proc Nat Acad Sci 97(10):5621–5626